


# Novel bilayer bacterial nanocellulose scaffold supports neocartilage formation in vitro and in vivo

## Journal Article

**Author(s):**

Martínez Ávila, Héctor; Feldmann, Eva-Maria; Pleumeekers, Mieke M.; Nimeskern, Luc; Kuo, Willy; de Jong, Willem C.; Schwarz, Silke; [Müller, Ralph](#) ; Hendriks, Jeanine; Rotter, Nicole; van Osch, Gerjo J. V. M.; Stok, Kathryn S.; Gatenholm, Paul

**Publication date:**

2015-03

**Permanent link:**

<https://doi.org/10.3929/ethz-a-010577251>

**Rights / license:**

[In Copyright - Non-Commercial Use Permitted](#)

**Originally published in:**

Biomaterials 44, <https://doi.org/10.1016/j.biomaterials.2014.12.025>

**Novel bilayer bacterial nanocellulose scaffold supports neocartilage formation *in vitro*  
and *in vivo***

Héctor Martínez Ávila<sup>1</sup>, Eva-Maria Feldmann<sup>2</sup>, Mieke M. Pleumeekers<sup>3</sup>, Luc Nimeskern<sup>4</sup>,  
Willy Kuo<sup>4</sup>, Willem C. de Jong<sup>5</sup>, Silke Schwarz<sup>2</sup>, Ralph Müller<sup>4</sup>, Jeanine Hendriks<sup>5</sup>, Nicole  
Rotter<sup>2</sup>, Gerjo J.V.M. van Osch<sup>3,6</sup>, Kathryn S. Stok<sup>4</sup> and Paul Gatenholm<sup>1\*</sup>

<sup>1</sup> *Biopolymer Technology, Department of Chemical and Biological Engineering, Chalmers  
University of Technology, Gothenburg, Sweden*

<sup>2</sup> *Department of Otorhinolaryngology, Ulm University Medical Center, Ulm, Germany*

<sup>3</sup> *Department of Otorhinolaryngology, Head and Neck Surgery, Erasmus MC, University  
Medical Center, Rotterdam, The Netherlands*

<sup>4</sup> *Institute for Biomechanics, ETH Zurich, Zurich, Switzerland*

<sup>5</sup> *CellCoTec BV, Bilthoven, The Netherlands*

<sup>6</sup> *Department of Orthopaedics, Erasmus MC, University Medical Center, Rotterdam, The  
Netherlands*

**Authors:**

Héctor Martínez Ávila

email: [hectorm@chalmers.se](mailto:hectorm@chalmers.se)

Eva-Maria Feldmann

email: [evamariafeldmann@yahoo.de](mailto:evamariafeldmann@yahoo.de)

Mieke M. Pleumeekers

email: [m.pleumeekers@erasmusmc.nl](mailto:m.pleumeekers@erasmusmc.nl)

Luc Nimeskern

email: [nluc@ethz.ch](mailto:nluc@ethz.ch)

Willy Kuo

email: [willykuo@gmx.ch](mailto:willykuo@gmx.ch)

Willem C. de Jong

email: [wilco.de.jong@cellcotec.com](mailto:wilco.de.jong@cellcotec.com)

---

**\* Corresponding author:**

Professor Paul Gatenholm

Biopolymer Technology, Department of Chemical and Biological Engineering  
Chalmers University of Technology

Kemivägen 4,

412 96 Gothenburg

Sweden

Tel.: +46 31 410461

Fax: +46 31 7723418

E-mail address: [paul.gatenholm@chalmers.se](mailto:paul.gatenholm@chalmers.se)

1 Silke Schwarz

2 email: [silke.schwarz@uniklinik-ulm.de](mailto:silke.schwarz@uniklinik-ulm.de)

3 Ralph Müller

4 email: [ram@ethz.ch](mailto:ram@ethz.ch)

5  
6  
7 Jeanine Hendriks

8 email: [Jeanine.Hendriks@cellcotec.com](mailto:Jeanine.Hendriks@cellcotec.com)

9  
10  
11 Nicole Rotter

12 email: [nicole.rotter@uniklinik-ulm.de](mailto:nicole.rotter@uniklinik-ulm.de)

13  
14 Gerjo JVM. van Osch

15 email: [g.vanosch@erasmusmc.nl](mailto:g.vanosch@erasmusmc.nl)

16  
17  
18 Kathryn S. Stok

19 email: [kstok@ethz.ch](mailto:kstok@ethz.ch)

20  
21  
22 Paul Gatenholm

23 email: [paul.gatenholm@chalmers.se](mailto:paul.gatenholm@chalmers.se)

24  
25  
26  
27  
28  
29  
30  
31  
32  
33  
34  
35  
36  
37  
38  
39  
40  
41  
42  
43  
44  
45  
46  
47  
48  
49  
50  
51  
52  
53  
54  
55  
56  
57  
58  
59  
60  
61  
62  
63  
64  
65

1  
2 **Abstract**

3  
4 Tissue engineering provides a promising alternative therapy to the complex surgical  
5  
6 reconstruction of auricular cartilage by using ear-shaped autologous costal cartilage. Bacterial  
7  
8 nanocellulose (BNC) is proposed as a promising scaffold material for auricular cartilage  
9  
10 reconstruction, as it exhibits excellent biocompatibility and secures tissue integration. Thus,  
11  
12 this study evaluates a novel bilayer BNC scaffold for auricular cartilage tissue engineering.  
13  
14 Bilayer BNC scaffolds, composed of a dense nanocellulose layer joined with a macroporous  
15  
16 composite layer of nanocellulose and alginate, were seeded with human nasoseptal  
17  
18 chondrocytes (NC) and cultured *in vitro* for up to 6 weeks. To scale up for clinical  
19  
20 translation, bilayer BNC scaffolds were seeded with a low number of freshly isolated  
21  
22 (uncultured) human NCs combined with freshly isolated human mononuclear cells (MNC)  
23  
24 from bone marrow in alginate and subcutaneously implanted in nude mice for 8 weeks. 3D  
25  
26 morphometric analysis showed that bilayer BNC scaffolds have a porosity of 75% and mean  
27  
28 pore size of  $50 \pm 25 \mu\text{m}$ . Furthermore, endotoxin analysis and *in vitro* cytotoxicity testing  
29  
30 revealed that the produced bilayer BNC scaffolds were non-pyrogenic ( $0.15 \pm 0.09 \text{ EU/ml}$ )  
31  
32 and non-cytotoxic (cell viability:  $97.8 \pm 4.7\%$ ). This study demonstrates that bilayer BNC  
33  
34 scaffolds offer a good mechanical stability and maintain a structural integrity while providing  
35  
36 a porous architecture that supports cell ingrowth. Moreover, bilayer BNC scaffolds provide a  
37  
38 suitable environment for culture-expanded NCs as well as a combination of freshly isolated  
39  
40 NCs and MNCs to form cartilage *in vitro* and *in vivo* as demonstrated by  
41  
42 immunohistochemistry, biochemical and biomechanical analyses.  
43  
44  
45  
46  
47  
48  
49  
50  
51  
52  
53  
54

55 **Keywords:** Tissue Engineering; Ear Cartilage; Neo-cartilage; Bacterial Nanocellulose;  
56  
57 Bacterial Cellulose; Nasoseptal Chondrocytes; Mononuclear Cells  
58  
59  
60  
61  
62  
63  
64  
65

## Introduction

Serious auricular defects such as anotia and microtia, along with auricle damage caused by cancer and trauma, demand an effective treatment for auricular cartilage reconstruction. For such cases, the field of tissue engineering (TE) provides a promising potential alternative therapy to the conventional and complex surgical reconstruction of auricular cartilage by using ear-shaped autologous costal and nasoseptal cartilage [1-3]. Bacterial nanocellulose (BNC), a novel biomaterial with excellent biocompatibility and remarkable tissue integration capability [4-8], has been evaluated for several TE strategies and has shown to support adhesion, proliferation and differentiation of different cell types [9-15]. BNC is a natural biopolymer synthesized by various bacteria species, particularly *Gluconacetobacter xylinus* [16, 17]. Its three-dimensional and interconnected network is composed of highly hydrated nanofibrils ranging from 70 to 140 nm in width, similar to collagen fibrils found in extracellular matrix (ECM) of several tissues, with high tensile strength [11, 18]. BNC is considered a hydrogel since it is mostly composed of water in its native state (99%). All together, these outstanding properties make BNC an exceptional biomaterial for many biomedical applications [19-21], including auricular cartilage reconstruction [8, 14, 22]. Although several groups have attempted to engineer auricular cartilage [1], few successful outcomes have been reported [23-25]. Development of artificial auricular grafts with adequate mechanical properties has been identified as a key factor for successful auricular cartilage TE [26]. Most studies that have used biodegradable scaffold materials have resulted in poor structural integrity (i.e. shape and size stability) of the auricular scaffold after implantation; caused by the short-lived chemical and mechanical stability [27-31]. On the other hand, recent studies that have investigated the use of non-degradable biomaterials for auricular cartilage reconstruction have reported a better structural integrity of the implant [23, 25, 32] – likely caused by the chemical stability of the support biomaterial, which translates

1 into long-lasting mechanical properties even after implantation. As opposed to the many  
2 biodegradable scaffolds previously evaluated for auricular cartilage TE, the long-term  
3 structural integrity of BNC scaffolds should not be compromised after implantation since  
4 humans do not produce enzymes capable of breaking down cellulose [33]. Besides being a  
5 chemically stable material, BNC with increased cellulose content of 17% (densified  
6 hydrogel) is a competitive scaffold material for repair, reconstruction or regeneration of  
7 auricular cartilage since it matches the elastic mechanical properties (e.g. equilibrium  
8 modulus) of human auricular cartilage [22], can be fabricated in patient-specific auricular  
9 shapes [34] and exhibits excellent biocompatibility *in vivo* - causing a minimal foreign body  
10 response [8].  
11  
12  
13  
14  
15  
16  
17  
18  
19  
20  
21  
22

23  
24 When densified, BNC hydrogel is a mechanically and biologically appropriate biomaterial  
25 for use in auricular cartilage reconstruction [8, 22]. However, its dense nanocellulose network  
26 prevents cells from penetrating the material. To circumvent this problem, several techniques  
27 have been developed to support cell ingrowth in BNC scaffolds by tuning pore size and pore  
28 interconnectivity during biosynthesis of BNC [35], via laser ablation [10] and freeze-dry  
29 processing [36, 37]. Such macroporous BNC scaffolds have been shown to provide an  
30 adequate environment that supports ingrowth and differentiation of chondrocytes. For  
31 example, human primary articular, auricular and nasoseptal chondrocytes cultured in  
32 macroporous BNC scaffolds *in vitro* have been shown to adhere, migrate, proliferate and  
33 maintain their chondrogenic phenotype – as confirmed by the synthesis of cartilage-specific  
34 ECM [14, 37, 38].  
35  
36  
37  
38  
39  
40  
41  
42  
43  
44  
45  
46  
47  
48  
49

50  
51 Engineering stable and functional auricular cartilage tissue also depends on the cell source  
52 used. Pleumeekers et al. showed that human auricular and nasoseptal chondrocytes possess a  
53 high chondrogenic capacity *in vivo*, making them attractive cell sources for auricular cartilage  
54 repair [39]. The use of cells in cartilage repair is an attractive strategy as it may result in  
55  
56  
57  
58  
59  
60  
61  
62  
63  
64  
65

1 regeneration of the lost tissue. However, the clinical application of a cell-aided treatment  
2 does feature challenges – a limited supply of autologous chondrocytes with the proper  
3 phenotype being the most stringent one. To cancel out cell culture, including the concomitant  
4 laboratory logistics and the double surgery, autologous cells should be isolated within the  
5 operating room and applied directly. In addition, the combination of chondrocytes with a less  
6 limited source of autologous cells, such as bone marrow mononuclear cells (MNC), can  
7 overcome the challenge of having too few cells and may even increase the treatment's  
8 performance [40, 41]. By resuspending the cells in alginate, also the factor of cell loss after  
9 scaffold seeding can be diminished whilst simultaneously providing the cells with a 3D  
10 environment to suppress dedifferentiation [42].

11 Several studies that have evaluated BNC as a scaffold material for auricular cartilage TE [8,  
12 14, 22, 37] have contributed to the design and development of BNC scaffolds with a two-  
13 layer (bilayer) architecture. This study investigates the *in vitro* and *in vivo* performance of  
14 bilayer BNC scaffolds, composed of a dense nanocellulose layer joined with a macroporous  
15 composite layer of nanocellulose and alginate, designed to be mechanically stable and  
16 maintain a long-term structural integrity while providing a porous architecture that supports  
17 cell ingrowth and neocartilage formation. Moreover, this study explores the application of a  
18 clinically relevant strategy by seeding a low number of freshly isolated (uncultured) human  
19 chondrocytes combined with freshly isolated human mononuclear cells, in order to test the  
20 translation of this auricular cartilage TE technology to the clinic.

## Materials and Methods

### Fabrication and purification of bilayer BNC scaffolds

#### *Production of dense and porous scaffold layers*

BNC hydrogel disks with increased cellulose content (i.e. dense layer) were produced and purified as described elsewhere [8]. Briefly, a suspension of *Gluconacetobacter xylinus* (ATCC<sup>®</sup> 700178, LGC Standards, Sweden) was inoculated in 250 ml conical flasks containing sterile culture medium (described by Matsuoka et al. [43]) and cultured at 30°C for 18 days, until large BNC cylinders (Ø 48 mm × 20 mm) were biosynthesized. The BNC cylinders were purified in a built-in-house perfusion system and compressed to 1 mm in height to increase the cellulose content. The compressed BNC pellicles were frozen to -80°C overnight and lyophilized (Heto PowerDry PL3000, Thermo Fisher Scientific, MA, USA) for 3 days. Dense BNC disks (Ø 8 mm × 1 mm) were then cut with a sterile biopsy punch (Miltex GmbH, Germany). The criterion for selecting the thickness of the dense BNC layer is based on morphometric analysis from MRI scans of human auricular cartilage, where Nimeskern et al. reported a cartilage thickness of  $1.15 \pm 0.10$  mm [44].

BNC/alginate composite scaffolds (i.e. porous layer) were fabricated by a freeze-drying process. First, purified BNC pellicles were homogenized with a blender, until a pulp consistency was obtained, and then with a dispersing element (S25N-18G, IKA, Germany) at 25,000 rpm for 20 minutes. Afterwards, the homogenized BNC suspension was steam sterilized (100 kPa, 121°C for 20 minutes) and the cellulose content was determined using a halogen moisture analyzer (HB43, Mettler-Toledo, OH, USA). The following steps were carried out in sterile conditions. The BNC suspension was mixed with 1.1% w/w clinical grade alginate dissolved in 0.9% NaCl (CellMed AG, Germany) to get a final composition of 90% dry weight BNC and 10% dry weight alginate compared to the total dry weight. The weight of alginate solution ( $W_{\text{Alg}}$ ) added to a known weight of BNC suspension ( $W_{\text{BNC}}$ ) was calculated by using the formula:  $W_{\text{Alg}} = W_{\text{BNC}} \times (\%DW_{\text{Alg}} \div \%DW_{\text{BNC}}) \times (\%CC_i \div \%AC_i)$ .



1  
2  
3  
4  
5  
6  
7  
8  
9  
10  
11  
12  
13  
14  
15  
16  
17  
18  
19  
20  
21  
22  
23  
24  
25  
26  
27  
28  
29  
30  
31  
32  
33  
34  
35  
36  
37  
38  
39  
40  
41  
42  
43  
44  
45  
46  
47  
48  
49  
50  
51  
52  
53  
54  
55  
56  
57  
58  
59  
60  
61  
62  
63  
64  
65

Where %DW<sub>Alg</sub> and %DW<sub>BNC</sub> are the targeted percent dry weight of alginate (10%) and BNC (90%) compared to the total dry weight; and %CC<sub>i</sub> and %AC<sub>i</sub> are the initial cellulose and alginate concentrations. The BNC/alginate mixture was then dispersed at 25,000 rpm for 15 minutes, transferred to sterile containers (TP52, Gosselin, France) and degassed in a vacuum desiccator. The containers were then placed inside Nalgene<sup>®</sup> cryo freezing containers (Thermo Fisher Scientific) and frozen to -80°C overnight at a rate of 1°C/min. The frozen BNC/alginate mixtures were lyophilized for 5 days to sublimate the ice crystals, creating a macroporous architecture. The dry BNC/alginate sponges were then sliced to 2 mm-thick slices and porous BNC/alginate composite scaffolds (Ø 8 mm × 2 mm) were cut with a sterile biopsy punch (Miltex GmbH).

#### ***Fabrication of bilayer BNC scaffolds***

A novel cellulose solvent system (i.e. ionic liquid EMIMAc) was used to attach the dense and porous layers and achieve a strong interfacial molecular bonding between the layers. The following steps were carried out in sterile conditions. First, dry homogenized BNC was dissolved in ionic liquid EMIMAc (1-ethyl-3-methylimidazolium acetate; Sigma-Aldrich, MO, USA) at a concentration of 10 mg/ml. The cellulose solvent solution was preheated to 80°C and then smeared on the dense BNC layers. Subsequently, the porous layers were aligned on top of the dense layers and the bilayer BNC scaffolds were placed on a heating plate at 80°C for 2 minutes to accelerate the dissolution of nanocellulose at the interface. The bilayer BNC scaffolds were then stabilized in 100 mM CaCl<sub>2</sub> in ethanol to precipitate the dissolved cellulose between the layers (i.e. attach the layers), while simultaneously crosslinking the alginate to bind the BNC in the porous layer. The scaffolds were then rehydrated and washed in non-pyrogenic conical tubes (TPP, Switzerland) with endotoxin-free water (HyClone<sup>™</sup> cell culture-grade water, Thermo Fisher Scientific) supplemented with 20 mM CaCl<sub>2</sub> to remove residuals of the ionic liquid EMIMAc and endotoxins. The scaffolds were purified under orbital motion (320 rpm) at 37°C for 14 days, during which the

1  
2  
3  
4  
5  
6  
7  
8  
9  
10  
11  
12  
13  
14  
15  
16  
17  
18  
19  
20  
21  
22  
23  
24  
25  
26  
27  
28  
29  
30  
31  
32  
33  
34  
35  
36  
37  
38  
39  
40  
41  
42  
43  
44  
45  
46  
47  
48  
49  
50  
51  
52  
53  
54  
55  
56  
57  
58  
59  
60  
61  
62  
63  
64  
65

endotoxin-free water and conical tubes were changed every second or third day.

Subsequently, the bilayer BNC scaffolds ( $\varnothing$  8 mm  $\times$  3 mm) were steam sterilized (as described above) in endotoxin-free water and stored until use at 4°C.

### **Characterization of bilayer BNC scaffolds**

The morphology of bilayer BNC scaffolds was characterized by scanning electron microscopy (SEM) and micro-computed tomography (microCT). Moreover, the purity of the bilayer BNC scaffolds was analyzed throughout the purification process by bacterial endotoxin testing, infrared spectroscopy analysis and *in vitro* cytotoxicity testing.

#### ***Scanning electron microscopy***

Samples were lyophilized (as described previously), thereafter sputter coated with a gold film and analyzed using a Leo Ultra 55 field emission gun (FEG) SEM (Carl Zeiss, Germany).

#### ***Micro-computed tomography***

Bilayer BNC scaffolds ( $n = 3$ ) were incubated in 0.1 M CaCl<sub>2</sub> solution at room temperature overnight and subsequently quenched in liquid nitrogen and lyophilized for 24 hours. The dry scaffolds were scanned with microCT ( $\mu$ CT50, Scanco Medical AG, Switzerland) at 45 kVp and 1  $\mu$ m nominal resolution. The internal microstructure of the porous layer was then segmented automatically using a constrained Gaussian filter to suppress noise and a global threshold (25% of maximal grayscale value). 3D morphometric parameters such as scaffold porosity (Sc.Po), volume-weighted mean pore size (Pore.Th), scaffold wall thickness (Wall.Th), and scaffold wall number (Wall.N) were calculated using the manufacturer's morphometry software (IPL, Scanco Medical AG) according to the guidelines established for the assessment of bone microstructure [45].

#### ***Bacterial endotoxin testing***

Endotoxin extraction from the bilayer BNC scaffolds was done in accordance to the international standard ISO 10993-12:2009 (Sample preparation and reference materials).

After 14 days of purification, bilayer BNC scaffolds ( $n=3$ ) were weighed and placed in

1 depyrogenated sample containers (Lonza, Belgium). Endotoxin-free water was added to the  
2 containers using the ratio of 0.1 grams of BNC/ml of extraction medium. The extraction was  
3 done at  $37 \pm 1^\circ\text{C}$  for  $72 \pm 2$  hours under orbital motion at 160 rpm. Endotoxin analysis was  
4 performed with the PyroGene<sup>TM</sup> Recombinant Factor C assay by Lonza. This assay has a  
5 minimum detection limit of 0.005 Endotoxin Units (EU) per milliliter. According to the USA  
6 Food and Drug Administration [46], endotoxin levels in medical devices are not to exceed  
7 0.5 EU/ml or 20 EU/device [46].

### 17 ***Attenuated Total Reflectance Fourier Transform Infrared (ATR-FTIR) spectroscopy***

18 Removal of EMIMAc residues from the bilayer BNC scaffolds was analyzed with ATR-  
19 FTIR spectroscopy. Samples ( $n=2$  per group) were freeze-dried after day 1, 7 and 14 of  
20 purification. The porous layer was removed from the bilayer BNC scaffolds to expose the  
21 interface. This interface, visible on the dense BNC layer, was analyzed with a single  
22 reflection ATR accessory fitted with a monolithic diamond crystal (GladiATR<sup>TM</sup>, Pike  
23 Technologies, WI, USA). The sample was placed on the small crystal area and a force was  
24 applied on the sample to push it onto the diamond surface. ATR-FTIR spectroscopy  
25 measurements were made with a System 2000 FT-IR spectrometer (PerkinElmer, MA, USA)  
26 in the mid-infrared region,  $4000$  to  $400\text{ cm}^{-1}$ . 20 scans were taken with a resolution of  $4\text{ cm}^{-1}$ .  
27 Pure EMIMAc solution and pure dried BNC films were used as controls.

### 43 ***In vitro cytotoxicity testing***

44 Removal of EMIMAc residues from the bilayer BNC scaffolds was also evaluated by *in vitro*  
45 cytotoxicity testing, according to the international standard ISO 10993-5:2009. Bilayer BNC  
46 scaffolds ( $n=4$  per time point) were incubated in growth medium (RPMI 1640 medium  
47 supplemented with 1% fetal bovine serum (FBS), and antibiotics (100 U/ml penicillin and  
48 100  $\mu\text{g/ml}$  streptomycin); Biochrom, Germany) for 24 hours to extract potential cytotoxic  
49 residues. All incubations were done in standard culture conditions ( $37^\circ\text{C}$ , 5%  $\text{CO}_2$  and 95%  
50 relative humidity). Meanwhile, sensitized L929 cells (ACC 2, DSMZ, Germany) were seeded  
51  
52  
53  
54  
55  
56  
57  
58  
59  
60  
61  
62  
63  
64  
65

1 in 96-well cell culture plates ( $1.0 \times 10^4$  cells per well) and incubated for 24 hours to allow  
2 cell adhesion. The medium was removed and 100  $\mu$ l of extract or control solutions was added  
3 to each well and incubated for 24 hours. Cell culture inserts (ThinCert™, Greiner BioOne,  
4 Germany) incubated in growth medium served as negative control ( $n=8$ ), while 10%  
5 dimethylsulfoxide in growth medium served as positive control ( $n=8$ ). After 24 hours of  
6 incubation in extract or control solutions, the medium was removed, 100  $\mu$ l medium were  
7 mixed with 20  $\mu$ l of CellTiter 96® AQueous one solution reagent (Promega, WI, USA) MTS  
8 and added to each well, followed by incubation for 2 hours at 37°C. Growth medium with  
9 reagent solution (without cells) served as blank ( $n=8$ ). After incubation with the reagent,  
10 absorbance was measured photometrically (Infinite M200 Pro, Tecan AG, Switzerland) at a  
11 wavelength of 490 nm and a reference wavelength of 680 nm. The average absorbance value  
12 of the negative control was used to compute the cell viability, where the negative control was  
13 regarded as 100% viability. The cytotoxic potential of the test samples was classified as  
14 highly cytotoxic when cell viability was below 50%, slightly cytotoxic when it was between  
15 51% and 70% and non-cytotoxic when cell viability was above 71%.

## 36 **Cell study I: performance of bilayer BNC scaffolds *in vitro***

### 37 ***Isolation and expansion of human nasoseptal chondrocytes***

38 Nasoseptal cartilage was obtained from 1 female patient (19 years) undergoing routine  
39 reconstructive septorhinoplasty at the Department of Otorhinolaryngology of Ulm University  
40 Medical Center (Ulm, Germany), as waste material after surgery, with approval of the local  
41 medical ethics committee (no. 152/08). The isolation of nasoseptal chondrocytes (NC) from  
42 the cartilage was done by enzymatic digestion of the tissue with 0.3% type II collagenase  
43 (Worthington Biochemical, NJ, USA) in growth medium (DMEM/Ham's F-12 supplemented  
44 with 10% FBS and 0.5% gentamycin; Biochrom) for 16 hours at 37°C under agitation. Cells  
45 were separated by filtration through a 100- $\mu$ m cell strainer and resuspended in growth  
46

1 medium. Subsequently, cell viability was determined using trypan blue staining and NCs  
2 were seeded in culture flasks at a density of 5,000 cells/cm<sup>2</sup> for expansion in monolayer  
3 culture. Once a cell confluence of about 85% was reached, the cells were trypsinized and  
4 cryopreserved.  
5  
6  
7

### 8 ***Cell culture of human chondrocytes in bilayer BNC scaffolds***

9 NCs were thawed and expanded one time in growth medium as described above. Once sub-  
10 confluent, cells were detached and resuspended in differentiation medium (NH ChondroDiff  
11 Medium; Miltenyi Biotec, Germany) supplemented with 0.5% gentamycin. Prior to cell  
12 seeding, bilayer BNC scaffolds ( $n=30$ ) were incubated in differentiation medium for 24  
13 hours. The medium was discarded and 50  $\mu$ l of cell suspension containing  $1.0 \times 10^6$  cells was  
14 seeded into the porous scaffold layer (10,000 cells/mm<sup>3</sup>). Cells were allowed to attach to the  
15 scaffolds for 4 hours in standard culture conditions (37°C, 5% CO<sub>2</sub> and 95% relative  
16 humidity), before transferring the seeded scaffolds to differentiation medium. Cell-seeded  
17 bilayer BNC scaffolds were cultured for up to 6 weeks and the medium was changed twice a  
18 week.  
19  
20  
21  
22  
23  
24  
25  
26  
27  
28  
29  
30  
31  
32  
33  
34  
35

### 36 ***Histological and immunohistochemical analyses***

37 During the *in vitro* culture, constructs were harvested weekly for qualitative evaluation of  
38 neocartilage synthesized by the chondrocytes. The constructs were fixed in 10% neutral  
39 buffered formalin solution supplemented with 20 mM CaCl<sub>2</sub> at room temperature overnight,  
40 embedded in paraffin and sectioned (5  $\mu$ m). For assessment of sulfated glycosaminoglycans  
41 (s-GAG) and cell distribution within the bilayer BNC scaffolds, longitudinal sections were  
42 stained with Alcian blue and counterstained with Mayer's hematoxylin. Furthermore, seeded  
43 scaffolds were processed for immunohistochemical (IHC) staining to detect cartilage specific  
44 proteins such as aggrecan (AB1031; Millipore, MA, USA), type II collagen (II-II6B3;  
45 DSHB, IA, USA) and the dedifferentiation marker type I collagen (ab34710; Abcam, UK).  
46  
47  
48  
49  
50  
51  
52  
53  
54  
55  
56  
57  
58  
59  
60  
61  
62  
63  
64  
65  
66  
67  
68  
69  
70  
71  
72  
73  
74  
75  
76  
77  
78  
79  
80  
81  
82  
83  
84  
85  
86  
87  
88  
89  
90  
91  
92  
93  
94  
95  
96  
97  
98  
99  
100  
101  
102  
103  
104  
105  
106  
107  
108  
109  
110  
111  
112  
113  
114  
115  
116  
117  
118  
119  
120  
121  
122  
123  
124  
125  
126  
127  
128  
129  
130  
131  
132  
133  
134  
135  
136  
137  
138  
139  
140  
141  
142  
143  
144  
145  
146  
147  
148  
149  
150  
151  
152  
153  
154  
155  
156  
157  
158  
159  
160  
161  
162  
163  
164  
165  
166  
167  
168  
169  
170  
171  
172  
173  
174  
175  
176  
177  
178  
179  
180  
181  
182  
183  
184  
185  
186  
187  
188  
189  
190  
191  
192  
193  
194  
195  
196  
197  
198  
199  
200  
201  
202  
203  
204  
205  
206  
207  
208  
209  
210  
211  
212  
213  
214  
215  
216  
217  
218  
219  
220  
221  
222  
223  
224  
225  
226  
227  
228  
229  
230  
231  
232  
233  
234  
235  
236  
237  
238  
239  
240  
241  
242  
243  
244  
245  
246  
247  
248  
249  
250  
251  
252  
253  
254  
255  
256  
257  
258  
259  
260  
261  
262  
263  
264  
265  
266  
267  
268  
269  
270  
271  
272  
273  
274  
275  
276  
277  
278  
279  
280  
281  
282  
283  
284  
285  
286  
287  
288  
289  
290  
291  
292  
293  
294  
295  
296  
297  
298  
299  
300  
301  
302  
303  
304  
305  
306  
307  
308  
309  
310  
311  
312  
313  
314  
315  
316  
317  
318  
319  
320  
321  
322  
323  
324  
325  
326  
327  
328  
329  
330  
331  
332  
333  
334  
335  
336  
337  
338  
339  
340  
341  
342  
343  
344  
345  
346  
347  
348  
349  
350  
351  
352  
353  
354  
355  
356  
357  
358  
359  
360  
361  
362  
363  
364  
365  
366  
367  
368  
369  
370  
371  
372  
373  
374  
375  
376  
377  
378  
379  
380  
381  
382  
383  
384  
385  
386  
387  
388  
389  
390  
391  
392  
393  
394  
395  
396  
397  
398  
399  
400  
401  
402  
403  
404  
405  
406  
407  
408  
409  
410  
411  
412  
413  
414  
415  
416  
417  
418  
419  
420  
421  
422  
423  
424  
425  
426  
427  
428  
429  
430  
431  
432  
433  
434  
435  
436  
437  
438  
439  
440  
441  
442  
443  
444  
445  
446  
447  
448  
449  
450  
451  
452  
453  
454  
455  
456  
457  
458  
459  
460  
461  
462  
463  
464  
465  
466  
467  
468  
469  
470  
471  
472  
473  
474  
475  
476  
477  
478  
479  
480  
481  
482  
483  
484  
485  
486  
487  
488  
489  
490  
491  
492  
493  
494  
495  
496  
497  
498  
499  
500  
501  
502  
503  
504  
505  
506  
507  
508  
509  
510  
511  
512  
513  
514  
515  
516  
517  
518  
519  
520  
521  
522  
523  
524  
525  
526  
527  
528  
529  
530  
531  
532  
533  
534  
535  
536  
537  
538  
539  
540  
541  
542  
543  
544  
545  
546  
547  
548  
549  
550  
551  
552  
553  
554  
555  
556  
557  
558  
559  
560  
561  
562  
563  
564  
565  
566  
567  
568  
569  
570  
571  
572  
573  
574  
575  
576  
577  
578  
579  
580  
581  
582  
583  
584  
585  
586  
587  
588  
589  
590  
591  
592  
593  
594  
595  
596  
597  
598  
599  
600  
601  
602  
603  
604  
605  
606  
607  
608  
609  
610  
611  
612  
613  
614  
615  
616  
617  
618  
619  
620  
621  
622  
623  
624  
625  
626  
627  
628  
629  
630  
631  
632  
633  
634  
635  
636  
637  
638  
639  
640  
641  
642  
643  
644  
645  
646  
647  
648  
649  
650  
651  
652  
653  
654  
655  
656  
657  
658  
659  
660  
661  
662  
663  
664  
665  
666  
667  
668  
669  
670  
671  
672  
673  
674  
675  
676  
677  
678  
679  
680  
681  
682  
683  
684  
685  
686  
687  
688  
689  
690  
691  
692  
693  
694  
695  
696  
697  
698  
699  
700  
701  
702  
703  
704  
705  
706  
707  
708  
709  
710  
711  
712  
713  
714  
715  
716  
717  
718  
719  
720  
721  
722  
723  
724  
725  
726  
727  
728  
729  
730  
731  
732  
733  
734  
735  
736  
737  
738  
739  
740  
741  
742  
743  
744  
745  
746  
747  
748  
749  
750  
751  
752  
753  
754  
755  
756  
757  
758  
759  
760  
761  
762  
763  
764  
765  
766  
767  
768  
769  
770  
771  
772  
773  
774  
775  
776  
777  
778  
779  
780  
781  
782  
783  
784  
785  
786  
787  
788  
789  
790  
791  
792  
793  
794  
795  
796  
797  
798  
799  
800  
801  
802  
803  
804  
805  
806  
807  
808  
809  
810  
811  
812  
813  
814  
815  
816  
817  
818  
819  
820  
821  
822  
823  
824  
825  
826  
827  
828  
829  
830  
831  
832  
833  
834  
835  
836  
837  
838  
839  
840  
841  
842  
843  
844  
845  
846  
847  
848  
849  
850  
851  
852  
853  
854  
855  
856  
857  
858  
859  
860  
861  
862  
863  
864  
865  
866  
867  
868  
869  
870  
871  
872  
873  
874  
875  
876  
877  
878  
879  
880  
881  
882  
883  
884  
885  
886  
887  
888  
889  
890  
891  
892  
893  
894  
895  
896  
897  
898  
899  
900  
901  
902  
903  
904  
905  
906  
907  
908  
909  
910  
911  
912  
913  
914  
915  
916  
917  
918  
919  
920  
921  
922  
923  
924  
925  
926  
927  
928  
929  
930  
931  
932  
933  
934  
935  
936  
937  
938  
939  
940  
941  
942  
943  
944  
945  
946  
947  
948  
949  
950  
951  
952  
953  
954  
955  
956  
957  
958  
959  
960  
961  
962  
963  
964  
965  
966  
967  
968  
969  
970  
971  
972  
973  
974  
975  
976  
977  
978  
979  
980  
981  
982  
983  
984  
985  
986  
987  
988  
989  
990  
991  
992  
993  
994  
995  
996  
997  
998  
999  
1000

1 antibodies. For aggrecan staining, slides were incubated in 0.5 U/ml chondroitinase ABC  
2 (Sigma-Aldrich) in PBS for 20 min at 32°C, followed by incubation with primary antibody  
3  
4 for 1 hour at a 1/100 dilution. For type II collagen staining, slides were incubated in 1%  
5  
6 hyaluronidase (Sigma-Aldrich) in PBS and 0.2% pronase (Calbiochem, Germany) in PBS,  
7  
8 each for 15 min at 37°C, followed by incubation with primary antibody for 1 hour at a 1/4000  
9  
10 dilution. For type I collagen staining, slides were incubated in proteinase K (Dako, Germany)  
11  
12 for 5 minutes at room temperature, followed by incubation with primary antibody for 1 hour  
13  
14 at a 1/400 dilution. For visualization of these markers, the LSAB+System-HRP kit (Dako),  
15  
16 which is based on the labeled streptavidin biotin method, was used according to the  
17  
18 manufacturer's protocol. Sections were counterstained with hematoxylin.  
19  
20  
21  
22  
23

### 24 ***Gene expression analysis***

25 Samples were harvested after 2, 4 and 6 weeks of *in vitro* culture, snap-frozen and stored at -  
26  
27 80°C until analyzed. For total RNA isolation, frozen constructs were placed in 2 ml  
28  
29 microcentrifuge tubes in quadruples and 100 µl of lysis buffer (10 µl β-Mercaptoethanol per  
30  
31 1 ml Buffer RLT; Qiagen, Germany) was added to each tube. The samples were disrupted  
32  
33 and homogenized for 2 minutes using a TissueLyser LT (Qiagen). Subsequently, 500 µl of  
34  
35 lysis buffer was added to each tube and the cell lysate was used for total RNA isolation using  
36  
37 RNeasy Mini Kit (Qiagen), according to manufacturer's protocol. Total RNA was quantified  
38  
39 using a multimode microplate reader (Infinite M200 Pro, Tecan AG) at 260/280 nm. cDNA  
40  
41 was synthesized from the extracted RNA using QuantiTect Reverse Transcription Kit  
42  
43 (Qiagen), according to manufacturer's protocol, in a PeqSTAR thermocycler (96 Universal  
44  
45 Gradient, PeqLab, Germany). For real-time two-step RT-PCR analysis, the sense and  
46  
47 antisense primers used are listed in Table 1. The following genes were analyzed: aggrecan  
48  
49 (*ACAN*), collagen type IIA1 (*COL2A1*), versican (*VCAN*) and collagen type IA1 (*COL1A1*).  
50  
51 Glyceraldehyde 3-phosphate dehydrogenase (*GAPDH*) was used as housekeeping gene. Real-  
52  
53 time two-step RT-PCR was performed using the Real Time ready RNA Virus Master assay  
54  
55  
56  
57  
58  
59  
60  
61  
62  
63  
64  
65

1 and LightCycler<sup>®</sup> 2.0 instrument (Roche, Germany). Relative gene expression levels were  
2 calculated by means of the  $2^{-\Delta CT}$  formula.  
3  
4

## 5 **Cell study II: performance of bilayer BNC scaffolds *in vivo***

### 6 ***Rapid isolation of human nasoseptal chondrocytes and bone marrow mononuclear cells***

7 Nasoseptal cartilage was obtained from male and female patients ( $n=47$ ; mean age 31 years;  
8 age range 18-69 years) undergoing routine reconstructive septorhinoplasty at the Department  
9 of Otorhinolaryngology of Ulm University Medical Center (Ulm, Germany) as waste  
10 material after surgery, with approval of the local medical ethics committee (no. 152/08). The  
11 collected nasoseptal cartilage was washed with PBS containing penicillin-streptomycin and  
12 stored in standard culture medium at 37°C, 5 % CO<sub>2</sub>, until further use. The 47 nasoseptal  
13 cartilage biopsies were divided in three pools for the chondrocyte isolations. Bone marrow  
14 aspirate was collected from three donors (mean age 70 years, 2 males, 1 female) during total  
15 hip replacement surgery, after acquiring written patient consent. The isolations of NCs from  
16 the cartilage and MNCs from the bone marrow were performed by CellCoTec (Bilthoven,  
17 The Netherlands). Patented clinically applied protocols were used to isolate the cells within  
18 the hour [41]. In brief, cartilage pieces were digested enzymatically under mechanical  
19 stimulation. Upon rapid digestion, any remaining debris was filtered out with a 100- $\mu$ m cell  
20 strainer. For the collection of MNCs, the bone marrow aspirate was relieved of its erythrocyte  
21 content using lysis buffer. Standard cell buffer was used for washing steps. Cell numbers and  
22 viability were measured using the Bürker-Türk method with trypan-blue exclusion.  
23  
24  
25  
26  
27  
28  
29  
30  
31  
32  
33  
34  
35  
36  
37  
38  
39  
40  
41  
42  
43  
44  
45  
46  
47

### 48 ***Seeding of bilayer BNC scaffolds with MNCs and NCs***

49 First, bilayer BNC scaffolds were freeze-dried in order to improve cell uptake during the cell  
50 seeding. To further improve the retention of cells in the scaffolds, cells were seeded in 1.1 %  
51 w/w alginate solution (CellMed AG). Cells encapsulated in alginate were then seeded in  
52 bilayer BNC scaffolds as a combination of 80% freshly isolated human MNCs and 20%  
53 freshly isolated human NCs at a total cell concentration of  $20 \times 10^6$  cells/ml alginate  
54  
55  
56  
57  
58  
59  
60  
61  
62  
63  
64  
65

1 (MNC/NC,  $n=4$ ). 200  $\mu$ l of the cell-alginate suspension was seeded into the porous layer of  
2 each scaffold. A cell-free alginate solution acted as a negative control (Cell-free,  $n=4$ ).  
3  
4 Subsequently, the alginate was instantaneously crosslinked with sterile 100 mM CaCl<sub>2</sub> for 10  
5 minutes and washed with 0.9% NaCl, followed by high glucose DMEM (Dulbecco's  
6  
7 Modified Eagle's Medium).  
8  
9

### 10 ***Subcutaneous implantation of constructs in mice***

11 To evaluate the stability of the bilayer BNC scaffolds and neocartilage formation *in vivo*,  
12 MNC/NC-seeded and cell-free bilayer BNC scaffolds were implanted subcutaneously on the  
13 dorsal side of 9-week-old nude female mice ( $n=2$ ; NMRI nu/nu, Charles River Laboratories,  
14 The Netherlands). Mice were placed under general anesthesia using 2.5% isoflurane. Two  
15 separate subcutaneous incisions of approximately 1 cm were made along the central line of  
16 the spine (1 at the shoulders and 1 at the hips), after which 4 separate subcutaneous pockets  
17 were prepared by blunt dissection of the subcutaneous tissue. The overall behavior and  
18 wound healing at the implant sites were assessed macroscopically over the implantation  
19 period. Eight weeks after subcutaneous implantation, animals were terminated and samples  
20 were explanted. Each sample was cut in half and one part was used for histology and the  
21 other part for biomechanical and biochemical analyses. Animal experiments were carried out  
22 with approval of the local Animal Experiments Committee of the Erasmus MC, Rotterdam,  
23 The Netherlands (EMC 2429).  
24  
25  
26  
27  
28  
29  
30  
31  
32  
33  
34  
35  
36  
37  
38  
39  
40  
41  
42  
43  
44

### 45 ***Histological and immunohistochemical analyses***

46 After 8 weeks of subcutaneous implantation, constructs were harvested, set in 2% agarose,  
47 fixed in 10% neutral buffered formalin solution, embedded in paraffin and sectioned (6  $\mu$ m).  
48 To examine proteoglycans present in the newly synthesized ECM, deparaffinized sections  
49 were stained with Safranin O and fast green. To allow the use of the monoclonal mouse  
50 antibody collagen type II (II-II6B3, 1:100; DSHB) on constructs which had been implanted  
51 in nude mice, we coupled the first and second antibody before applying them on the sections  
52  
53  
54  
55  
56  
57  
58  
59  
60  
61  
62  
63  
64  
65



1 to prevent unwanted binding of the anti-mouse antibodies to mouse immunoglobulins, as  
2 described previously [47]. In short, the primary antibody was pre-coupled overnight with  
3 goat anti-mouse biotin at 4°C (1:500; Jackson Laboratories, ME, USA), followed by a 2 hour  
4 incubation in 0.1% normal mouse serum (CLB, The Netherlands) in order to capture the  
5 unbound second antibody. Antigen retrieval was performed through incubation with 0.1%  
6 pronase (Sigma-Aldrich) in PBS for 30 minutes at 37°C, followed by a 30 minute incubation  
7 with 1% hyaluronidase (Sigma-Aldrich) in PBS at 37°C. Non-specific binding sites were  
8 blocked with 10% goat serum (Sigma-Aldrich) in PBS and sections were stained with the  
9 pre-treated antibodies for 60 minutes. Sections were then incubated with enzyme-streptavidin  
10 conjugate (1:100; Biogenex, California, USA) in PBS/1% BSA, followed by incubation with  
11 Neu Fuchsin substrate (Chroma, Germany). Positive staining for type II collagen was  
12 confirmed with the use of native ear cartilage. A monoclonal mouse IgG1 antibody (X0931;  
13 Dako) was used as a negative control.

### 31 ***Biochemical analysis***

32 Sulfated glycosaminoglycans (s-GAG) were quantified using the 1,9-dimethylmethylene blue  
33 (DMMB) dye-binding assay. First, alginate was dissolved in 55 mM sodium citrate and  
34 digested overnight at 56°C in papain (250 µg/ml in 0.2 M NaH<sub>2</sub>PO<sub>4</sub>, 0.01 M EDTA,  
35 containing 5 mM L-cysteine; pH 6.0). To be suitable for cell cultures containing alginate, the  
36 DMMB-pH-level was decreased to pH 1.75, as described previously [48]. The metachromatic  
37 reaction of DMMB was monitored using a spectrophotometer. Absorption ratios of 540 and  
38 595 nm were used to determine the GAG content with chondroitin sulfate C derived from  
39 shark (Sigma-Aldrich) as a standard. The amount of GAG was expressed per tissue wet  
40 weight ( $n=4$ ).

### 54 ***Biomechanical analysis***

55 Mechanical properties of the retrieved constructs ( $n=8$ , MNC/NC-seeded and cell-free  
56 scaffolds) and non-implanted bilayer BNC scaffolds containing cell-free alginate solution  
57  
58  
59  
60  
61  
62  
63  
64  
65

1 (n=5, non-implanted group) were assessed with uniaxial materials testing machine (Z005,  
2 Zwick GmbH, Germany) equipped with a 10 N load cell, a cylindrical plane-ended stainless  
3 steel indenter ( $\varnothing$  0.35 mm) and a built-in displacement control. Bilayer BNC scaffolds were  
4 placed in close-fitting stainless steel cylindrical wells containing PBS supplemented with 1%  
5 antibiotic/antimycotic solution. Stress relaxation testing was performed as described  
6  
7 previously [49]. Briefly, a preload of 3 mN was first applied on the sample to locate the  
8 sample surface and measure sample thickness, and held for 5 minutes. Five successive strain  
9 steps were then applied in 5% increments of the original sample thickness, and specimens  
10 were left to relax for 20 minutes at each step. The hold time was defined as the time  
11 necessary to reach equilibrium. Two locations were tested on each sample (center of the  
12 sample, and 1.2 mm off-center). Measurements of maximum stress ( $\sigma_{\max}$ ), instantaneous  
13 modulus ( $E_{\text{in}}$ ) and equilibrium modulus ( $E_{\text{eq}}$ ) were computed from the stress-strain curves,  
14 which are normalized for sample thickness. Additionally, a relaxation half-life time ( $t_{1/2}$ ),  
15 defined as the time needed for the stress to decrease to half of its maximum value, was  
16 computed to estimate the viscoelastic relaxation after the first strain application, as described  
17 previously [22].  
18  
19  
20  
21  
22  
23  
24  
25  
26  
27  
28  
29  
30  
31  
32  
33  
34  
35  
36  
37  
38  
39

### 40 **Statistical analysis**

41 Statistical analyses were performed with Statgraphics Centurion Version 17 (Statpoint  
42 Technologies, VA, USA). For cytotoxicity analysis, comparison of means was assessed by  
43 one-way ANOVA, followed by Tukey's HSD test for post hoc comparisons. For biochemical  
44 analysis, a two-sample Kolmogorov-Smirnov test was performed for comparing two groups.  
45  
46 For biomechanical analysis, comparison of means was assessed by one-way ANOVA and  
47 Tukey's HSD test. When the data did not meet the requirements for a parametric test, a  
48 Kruskal-Wallis test was performed, followed by the Mann-Whitney test for post hoc  
49  
50  
51  
52  
53  
54  
55  
56  
57  
58  
59  
60  
61  
62  
63  
64  
65

comparisons. Values of  $p < 0.05$  were considered statistically significant. The mean and standard deviation (SD) are presented.

1  
2  
3  
4  
5  
6  
7  
8  
9  
10  
11  
12  
13  
14  
15  
16  
17  
18  
19  
20  
21  
22  
23  
24  
25  
26  
27  
28  
29  
30  
31  
32  
33  
34  
35  
36  
37  
38  
39  
40  
41  
42  
43  
44  
45  
46  
47  
48  
49  
50  
51  
52  
53  
54  
55  
56  
57  
58  
59  
60  
61  
62  
63  
64  
65

## Results

### Production and morphological characterization of bilayer BNC scaffolds

Bilayer BNC scaffolds, composed of a dense nanocellulose layer joined with a macroporous composite layer of nanocellulose and alginate, were successfully fabricated (Figures 1 and 2). The dense and porous layers were stable and firmly attached, which facilitated the handling of the scaffolds during the purification process and throughout the study. SEM images revealed a compact BNC network structure in the dense layer and a macroporous structure in the porous layer. However, information about the pore size distribution was not possible to extract from these images (Figure 2b, c). Scanning and reconstruction with microCT of the micro- and macro-structures of the porous layer allowed computation of the 3D morphometric parameters by distance transformation. The Sc.Po, Pore.Th, Wall.Th and Wall.N of a typical porous layer of a BNC bilayer scaffold was 75%,  $50 \pm 25 \mu\text{m}$ ,  $18 \pm 10 \mu\text{m}$  and  $21 \text{ mm}^{-1}$ , respectively (Figure 2f, g).

### Purification of bilayer BNC scaffolds

The bilayer BNC scaffolds were successfully purified from endotoxins, as shown by the low endotoxin level ( $0.15 \pm 0.09 \text{ EU/ml}$ ) found after 14 days of washing with endotoxin-free water (Table 2). This value is three times lower than the endotoxin limit ( $0.5 \text{ EU/ml}$ ) set by the FDA for medical devices [46]. The result from endotoxin analysis verified the effectiveness of the purification process to remove endotoxins from the bilayer BNC scaffolds. The removal of EMIMAc residues from the bilayer BNC scaffolds was analyzed with ATR-FTIR spectroscopy. The strong peak at wavenumber  $1566 \text{ cm}^{-1}$ , observed in the ATR spectrum of EMIMAc solution, was used to detect EMIMAc residues in the ATR spectra of bilayer BNC scaffolds. This peak is composed of two overlapped peaks that correspond to the carboxyl group of the acetate and an underlying ring mode of the cation, as shown by previous studies [50, 51]. A small peak at  $1566 \text{ cm}^{-1}$  was also found in the ATR

1 spectra of bilayer BNC scaffolds after 1 and 7 days of purification. However, the absence of  
2 the peak at  $1566\text{ cm}^{-1}$  in the ATR spectra of samples that were washed for 14 days confirmed  
3 the removal of EMIMAc residues from the bilayer BNC scaffolds (Figure 3a). *In vitro*  
4 cytotoxicity testing supported this observation.  
5  
6

7  
8  
9 A one-way ANOVA was conducted to compare the effect of cytotoxic residues extracted  
10 from BNC bilayer scaffolds (i.e. at 7 and 14 days of purification) and control conditions on  
11 cell viability. There was a significant effect of extracted cytotoxic residues on levels of cell  
12 viability for the four conditions,  $F(3, 20) = 120.42, p < 0.0001, \omega = 0.97$ . Post hoc  
13 comparisons using the Tukey HSD test indicated that the mean cell viability for the 14-day  
14 condition ( $97.8 \pm 4.7\%$ ) was significantly higher than the 7-day ( $18.4 \pm 3.6\%$ ) and positive  
15 control conditions ( $25.6 \pm 5.5\%$ ) at the  $p < 0.05$  level. Furthermore, there was no significant  
16 difference between the negative control and 14-day conditions. Thus, the cytotoxic potential  
17 of bilayer BNC scaffolds, after 14 days of washing with endotoxin-free water, was classified  
18 as non-cytotoxic (cell viability  $> 71\%$ ) (Figure 3b).  
19  
20  
21  
22  
23  
24  
25  
26  
27  
28  
29  
30  
31  
32  
33

### 34 **Performance of bilayer BNC scaffolds and neocartilage formation *in vitro***

35 Gross examination of the cell-seeded constructs throughout the 6 weeks of cell culture  
36 revealed that the adhesion between the dense support layer and porous layer remained good.  
37  
38 Moreover, the size and shape of the bilayer BNC scaffolds remained stable during the cell  
39 culture. Deposition of ECM by the NCs seeded in bilayer BNC scaffolds was assessed  
40 qualitatively by immunohistological staining. During 3D culture, NCs produced and  
41 accumulated cartilage-specific ECM components in the bilayer BNC scaffolds. A positive  
42 staining for s-GAGs was found around clusters of chondrocytes in the porous layer after 2  
43 weeks of culture, as shown by the Alcian blue staining (Figure 4a). Moreover, synthesis and  
44 accumulation of s-GAGs, aggrecan as well as type II collagen increased visibly during 3D  
45 culture (Figure 4a-c). After 6 weeks of 3D culture, a homogeneous production of  
46  
47  
48  
49  
50  
51  
52  
53  
54  
55  
56  
57  
58  
59  
60  
61  
62  
63  
64  
65

1 chondrogenic ECM was observed throughout the porous layer, even at the center. However,  
2 fibrocartilage ECM was also synthesized by the NCs in the bilayer BNC scaffolds, as  
3 demonstrated by the positive immunostaining of type I collagen (Figure 4d).  
4

5  
6  
7 The capacity of NCs to synthesize cartilage-specific ECM components when seeded in the  
8 BNC scaffold was also investigated on the basis of the expression of the chondrogenic  
9 marker genes *ACAN* and *COL2A1*. To assess whether the NCs were able to redifferentiate  
10 and maintain their chondrogenic phenotype, the expression not only of the chondrogenic  
11 markers but also of the dedifferentiation markers, *VCAN* and *COL1A1*, was determined. Gene  
12 expression analyses confirmed the positive immunostains of aggrecan, type II and type I  
13 collagen. NCs cultured in bilayer BNC scaffolds were able to express *ACAN* and *COL2A1*.  
14

15  
16  
17 The expression of both chondrogenic markers increased clearly during 3D culture for up to 6  
18 weeks. *ACAN* and *COL2A1* expression after 6 weeks was 3.4- and 4.9-fold higher,  
19 respectively, compared to gene expression levels at week 2. Expression of *COL1A1* was also  
20 upregulated during 3D culture, where after 6 weeks was 1.7-fold higher compared to gene  
21 expression levels at week 2. On the other hand, expression of *VCAN* remained relatively  
22 close to zero during the 6 weeks of 3D culture (Figure 4e, f). The upregulation of the  
23 chondrogenic markers *ACAN* and *COL2A1* was clearly enhanced compared to the expression  
24 of dedifferentiation markers, revealing the chondrogenic potential of the NCs in the bilayer  
25 BNC scaffolds.  
26

27  
28  
29 Cell ingrowth and cell distribution in the bilayer BNC scaffolds were also assessed by  
30 histological analysis. As demonstrated in figure 4a, the porous layer supported the ingrowth  
31 of NCs and facilitated a homogeneous cell distribution. However, it took 4 weeks of *in vitro*  
32 culture to get a dense and homogenous cell distribution since there was a substantial loss of  
33 cells after seeding in medium. As a means to increase the number of cells retained in the  
34  
35  
36  
37  
38  
39  
40  
41  
42  
43  
44  
45  
46  
47  
48  
49  
50  
51  
52  
53  
54  
55  
56  
57  
58  
59  
60  
61  
62  
63  
64  
65

1 scaffolds, cells were seeded in alginate solution. This significantly improved cell retention in  
2 the scaffolds, even after 1 day of seeding (data not shown).  
3  
4

### 5 **Performance of bilayer BNC scaffolds and neocartilage formation *in vivo***

6 The stability and neocartilage formation in MNC/NC-seeded and cell-free bilayer BNC  
7 scaffolds were evaluated after 8 weeks of subcutaneous implantation in nude mice. The mice  
8 survived until the end of the study period, during which no extrusion of constructs was  
9 observed. At 8 weeks post-implantation, a thin fibrous capsule surrounded all MNC/NC-  
10 seeded and cell-free bilayer BNC scaffolds – considered a normal non-pathological foreign  
11 body reaction. Macroscopic examination of the explants revealed that the shape and size of  
12 the bilayer BNC scaffolds remained stable and no delamination of the dense and porous  
13 layers was observed in any of the constructs. Furthermore, bilayer BNC scaffolds seeded with  
14 MNCs and NCs encapsulated in alginate had a macroscopically cartilage-like appearance.  
15 These MNC/NC-seeded constructs were stiffer and more stable upon handling, compared to  
16 bilayer BNC scaffolds seeded with cell-free alginate solution. The cells encapsulated in  
17 alginate were homogeneously distributed in the porous layer of the scaffolds at 8 weeks post-  
18 implantation, as observed by the histology images (Figure 5b, c).  
19  
20  
21  
22  
23  
24  
25  
26  
27  
28  
29  
30  
31  
32  
33  
34  
35  
36  
37  
38

39 Proteoglycan synthesis was examined using a Safranin O staining. As expected, no positive  
40 stain for Safranin O was found in the cell-free bilayer BNC scaffolds. Depositions of  
41 proteoglycans were observed in the MNC/NC-seeded bilayer BNC scaffolds after 8 weeks of  
42 subcutaneous implantation, as shown by the strong Safranin O stain surrounding the cells  
43 (Figure 5b). The results pointing towards chondrogenic ECM produced by the cells in the  
44 bilayer BNC scaffolds were confirmed by the positive immunostaining of type II collagen,  
45 which was intensely stained in areas of the construct (Figure 5c). Moreover, a Kolmogorov-  
46 Smirnov test indicated a significant difference ( $p < 0.05$ ) between mean GAG content for  
47 MNC/NC-seeded ( $0.87 \pm 0.65 \mu\text{g GAG/mg wet weight}$ ) and cell-free bilayer BNC scaffolds  
48  
49  
50  
51  
52  
53  
54  
55  
56  
57  
58  
59  
60  
61  
62  
63  
64  
65

1  
2  
3  
4  
5  
6  
7  
8  
9  
10  
11  
12  
13  
14  
15  
16  
17  
18  
19  
20  
21  
22  
23  
24  
25  
26  
27  
28  
29  
30  
31  
32  
33  
34  
35  
36  
37  
38  
39  
40  
41  
42  
43  
44  
45  
46  
47  
48  
49  
50  
51  
52  
53  
54  
55  
56  
57  
58  
59  
60  
61  
62  
63  
64  
65

( $0.07 \pm 0.11 \mu\text{g GAG/mg wet weight}$ ). GAG-production in the MNC/NC group was almost 12-fold higher compared to the control condition (Figure 5d).

### ***Biomechanical analysis***

A typical stress relaxation behavior was observed in all bilayer BNC scaffolds (MNC/NC-seeded and cell-free controls), and the following measurements were determined for the MNC/NC-seeded constructs at 8 weeks post-implantation;  $0.76 \pm 0.19 \text{ MPa}$  for  $E_{\text{in}}$ ,  $0.19 \pm 0.08 \text{ MPa}$  for  $E_{\text{eq}}$ ,  $0.16 \pm 0.07 \text{ MPa}$  for  $\sigma_{\text{max}}$  and  $7.1 \pm 3.4 \text{ seconds}$  for  $t_{1/2}$ . A one-way ANOVA was conducted to compare the effect of implantation and seeding of MNC/NCs on initial matrix stiffness (i.e.  $E_{\text{in}}$ ) of the constructs at 8 weeks post-implantation. There was a significant effect of implantation and seeding of MNC/NCs on instantaneous modulus for the three conditions,  $F(2, 23) = 16.10, p < 0.0001, \omega = 0.73$ . Post hoc comparisons using the Tukey HSD test indicated that the mean  $E_{\text{in}}$  for the MNC/NC condition ( $0.76 \pm 0.19 \text{ MPa}$ ) was significantly higher than the non-implanted ( $0.42 \pm 0.15 \text{ MPa}$ ) and cell-free conditions ( $0.32 \pm 0.10 \text{ MPa}$ ) at the  $p < 0.05$  level. The cell-free implanted condition did not significantly differ from the non-implanted condition (Figure 5e).

Moreover, a Kruskal–Wallis test was conducted to compare the effect of implantation and seeding of MNC/NCs on relaxation kinetics (i.e.  $t_{1/2}$ ) and intrinsic properties (i.e.  $E_{\text{eq}}$  and  $\sigma_{\text{max}}$ ) of the constructs at 8 weeks post-implantation. The median  $t_{1/2}$  values of the constructs were significantly affected by the implantation and seeding of MNC/NCs,  $H(2) = 17.46, p < 0.001$ . However,  $E_{\text{eq}}$  and  $\sigma_{\text{max}}$  were not significantly affected by the tested conditions,  $H(2) = 4.19, p = 0.12$  and  $H(2) = 1.12, p = 0.57$ , respectively. Post hoc comparisons using the Mann–Whitney tests indicated that the median  $t_{1/2}$  for the MNC/NC condition was significantly higher than the non-implanted ( $U = 3, p < 0.001, r = -0.74$ ) and cell-free conditions ( $U = 48, p < 0.01, r = -0.66$ ). No significant differences in  $t_{1/2}$  were detected between the cell-free and non-implanted conditions. A 2.4- and 3.4-fold higher  $E_{\text{in}}$  and  $t_{1/2}$ , respectively, were observed in the MNC/NC-seeded constructs compared to the cell-free



group. Likewise, a 1.8- and 3.6-fold higher  $E_{in}$  and  $t_{1/2}$ , respectively, was observed in the MNC/NC-seeded constructs compared to the non-implanted group (Figure 5e).

1  
2  
3  
4  
5  
6  
7  
8  
9  
10  
11  
12  
13  
14  
15  
16  
17  
18  
19  
20  
21  
22  
23  
24  
25  
26  
27  
28  
29  
30  
31  
32  
33  
34  
35  
36  
37  
38  
39  
40  
41  
42  
43  
44  
45  
46  
47  
48  
49  
50  
51  
52  
53  
54  
55  
56  
57  
58  
59  
60  
61  
62  
63  
64  
65

## Discussion

1  
2 A novel bilayer BNC scaffold was successfully evaluated for auricular cartilage TE. This  
3  
4 study demonstrates that non-pyrogenic and non-cytotoxic bilayer BNC scaffolds offer a good  
5  
6 mechanical stability and maintain a structural integrity while providing a porous architecture  
7  
8 that supports cell ingrowth. Moreover, bilayer BNC scaffolds, together with alginate, provide  
9  
10 a suitable environment for human nasoseptal chondrocytes to form cartilage.  
11  
12

13  
14 As shown by the endotoxin analysis, the purification process reduced the endotoxins in the  
15  
16 bilayer BNC scaffolds to a level well below the endotoxin limit set by the FDA for medical  
17  
18 devices [46]. This low endotoxin content ( $0.15 \pm 0.09$  EU/ml) found in the bilayer BNC  
19  
20 scaffolds is in good agreement with our previous results (0.10 EU/ml, [8]), where densified  
21  
22 BNC hydrogel disks (i.e. dense layer) of similar dimensions were considered non-pyrogenic  
23  
24 after purification with endotoxin-free water for 14 days.  
25  
26

27  
28 The ionic liquid EMIMAc offers a novel cellulose solvent system to achieve a strong  
29  
30 interfacial molecular bonding between the cellulosic dense and porous layers. We are not  
31  
32 aware of any other methods that can achieve such result. On the other hand, using EMIMAc  
33  
34 increases the risk of having cytotoxic compounds in the bilayer BNC scaffolds, if these  
35  
36 residues are not properly removed during the purification process. Since the toxicity of ionic  
37  
38 liquids is not well understood, the use of EMIMAc to fabricate the bilayer BNC scaffolds  
39  
40 was investigated with precaution. The cytotoxicity of imidazole ionic liquids has been studied  
41  
42 in a human lung carcinoma epithelial cell line model, and it was found that the alkyl-chain  
43  
44 length of the ionic liquid has an influence on cytotoxicity [52]. However, the cytotoxicity of  
45  
46 EMIMAc, in particular, has not been studied in eukaryotes. Consequently, we analyzed the  
47  
48 removal of EMIMAc from the bilayer BNC scaffolds with ATR-FTIR spectroscopy,  
49  
50 followed by *in vitro* cytotoxicity testing with sensitized L929 cells. The strong peak at  
51  
52 wavenumber  $1566\text{ cm}^{-1}$  was used to detect EMIMAc residues in the ATR spectra of bilayer  
53  
54  
55  
56  
57  
58  
59  
60  
61  
62  
63  
64  
65

1 BNC scaffolds, as it has been shown that this peak is composed of two overlapped peaks that  
2 correspond to the carboxyl group of the acetate and an underlying ring mode of the cation  
3  
4 [50, 51]. Since the peak at  $1566\text{ cm}^{-1}$  was found in the ATR spectra of bilayer BNC scaffolds  
5  
6 that had been washed for 1 and 7 days, it was considered necessary to continue washing the  
7  
8 scaffolds in endotoxin-free water. The washing process proved to be successful in removing  
9  
10 the EMIMAc residues, as first observed in the ATR spectra of samples that were washed for  
11  
12 14 days. The absence of this peak confirmed the removal of EMIMAc from the BNC bilayer  
13  
14 scaffolds.  
15  
16

17  
18  
19 *In vitro* cytotoxicity testing supported our findings from ATR-FTIR. Bilayer BNC scaffolds  
20  
21 washed for 7 days still had residues of EMIMAc that were highly cytotoxic to L929 cells  
22  
23 (cell viability:  $18.4 \pm 3.6\%$ ). However, these residues were further reduced after the  
24  
25 purification process with endotoxin-free water; yielding non-cytotoxic bilayer BNC  
26  
27 scaffolds. These results are in good agreement with our previous study which evaluated the  
28  
29 cytotoxic potential of pure densified BNC hydrogel disks (i.e. dense layer) and found the  
30  
31 material to be non-cytotoxic [8]. All together, the results from ATR-FTIR and *in vitro*  
32  
33 cytotoxicity testing demonstrated that EMIMAc residues were successfully removed from the  
34  
35 bilayer BNC scaffolds after the purification process with endotoxin-free water; whereat no  
36  
37 peak at  $1566\text{ cm}^{-1}$  and no cytotoxic effects were observed.  
38  
39

40  
41  
42  
43 Macroscopic examination of the bilayer BNC scaffolds after the *in vitro* and *in vivo* studies  
44  
45 revealed that the adhesion between the dense and porous layers remained stable, as there  
46  
47 were no signs of adhesive failure. We postulate that the interfacial bonding between the  
48  
49 layers is like a molecular welding process. As the BNC-EMIMAc solution partly dissolves  
50  
51 both surfaces at the interface, this makes it possible for the long chains of BNC to diffuse into  
52  
53 both layers. Once the dissolved BNC is precipitated in ethanol, the interface structure is  
54  
55 locked, which results in a stable interfacial bonding. We have observed that when pulling the  
56  
57  
58  
59  
60  
61  
62  
63  
64  
65

1 dense and porous layers apart, the scaffold breaks at the porous layer, similar to a structural  
2 failure. In contrast, a weak adhesion would have had resulted in an adhesive or cohesive  
3 failure at the interface. Based on this observation we speculate that the interfacial bonding  
4 between the layers is stronger than the structure of the porous layer, although in this study the  
5 interfacial strength of the bilayer BNC scaffolds was not measured.  
6  
7  
8  
9

10 The compact BNC network structure of the dense layer provided a good mechanical stability,  
11 while the interconnected high porosity layer (75% porosity with mean pore size of  $50 \pm 25$   
12  $\mu\text{m}$ ) supported the ingrowth and homogeneous distribution of NCs throughout this layer. In  
13 agreement with our previous study, which evaluated BNC/alginate composite scaffolds *in*  
14 *vitro* [37], bilayer BNC scaffolds also supported the redifferentiation of NCs to a more  
15 chondrogenic phenotype, which led to the formation of neocartilage; as demonstrated by the  
16 increase in gene expression of chondrogenic marker genes *ACAN* and *COL2A1* and  
17 homogeneous distribution of cartilage-specific ECM after 6 weeks of *in vitro* culture.  
18  
19  
20  
21  
22  
23  
24  
25  
26  
27  
28  
29  
30

31 Although, the expression of dedifferentiation marker *VCAN* remained constantly low, a  
32 strong expression of *COL1A1* was observed during the *in vitro* culture. The presence of  
33 *COL2A1* and *COL1A1* indicates a subpopulation of NCs that did not switch to a  
34 chondrogenic phenotype during 3D culture in bilayer BNC scaffolds under chondrogenic  
35 medium conditions.  
36  
37  
38  
39  
40  
41  
42  
43

44 After 6 weeks of *in vitro* culture, a rich and homogenous distribution of cells and neocartilage  
45 was observed throughout the porous layer of the scaffold, even in the center, which is known  
46 to be a critical region in static 3D culture due to the limited supply of nutrients and oxygen.  
47  
48  
49  
50

51 This outcome could have been accelerated by increasing the percentage of cells retained in  
52 the scaffolds after cell seeding, as there was a substantial loss of cells when these were  
53 seeded in medium. Embedding the cells in alginate significantly improved cell retention in  
54 the scaffolds after seeding. Alginate was chosen, since it has been successfully used to seed  
55  
56  
57  
58  
59  
60  
61  
62  
63  
64  
65

1 chondrocytes in a scaffold for *in vivo* implantation [53, 54] and this hydrogel is well known  
2 to maintain a chondrogenic phenotype of human chondrocytes and stimulate neocartilage  
3 formation [42].  
4

5  
6  
7 In the *in vivo* study we explored the application of a clinically relevant strategy, by seeding  
8 bilayer BNC scaffolds with a low number of freshly isolated human chondrocytes combined  
9 with freshly isolated human mononuclear cells, in order to test the translation of this auricular  
10 cartilage TE technology to the clinic. At 8 weeks post-implantation, deposition of cartilage  
11 matrix components such as proteoglycan and type II collagen were observed predominantly  
12 in MNC/NC-seeded constructs. The strong Safranin O stain surrounding the cells showed the  
13 presence of proteoglycans in the newly synthesized ECM, while the presence of type II  
14 collagen was confirmed by immunohistochemistry. These results, showing the formation of  
15 neocartilage in the porous layer, were further confirmed by biochemical analysis; where  
16 GAG-production in the MNC/NC-seeded bilayer BNC scaffolds was significantly higher  
17 than the control condition (12-fold).  
18  
19  
20  
21  
22  
23  
24  
25  
26  
27  
28  
29  
30  
31  
32

33  
34 The presence of cartilage matrix in the bilayer BNC scaffolds was also supported by  
35 biomechanical analysis. At 8 weeks post-implantation, a significantly higher initial matrix  
36 stiffness and improved relaxation kinetics (i.e. higher  $E_{in}$  and  $t_{1/2}$  values) were observed in the  
37 MNC/NC-seeded scaffolds compared to the non-implanted and cell-free conditions. In fact,  
38 the effect size (i.e.  $\omega$  and  $r > 0.5$ ) obtained from the  $E_{in}$  and  $t_{1/2}$  data represents a large effect  
39 by the MNC/NC condition. However, there was no significant difference in  $E_{eq}$  and  $\sigma_{max}$  for  
40 the three conditions. Considering the improved relaxation kinetics in the MNC/NC-seeded  
41 constructs, we conclude that the ability of the MNC/NC-seeded scaffolds to attract and trap  
42 water was enhanced through the production and accumulation of proteoglycans and  
43 glycosaminoglycans in the bilayer BNC scaffolds. Nevertheless, since the intrinsic scaffold  
44 properties did not improve in the MNC/NC-seeded constructs compared to the no cell control  
45  
46  
47  
48  
49  
50  
51  
52  
53  
54  
55  
56  
57  
58  
59  
60  
61  
62  
63  
64  
65

1 (no difference in  $E_{eq}$ ), it implies that collagen matrix was not effectively produced in the  
2 porous layer. To put the results from the biomechanical analysis in a clinical context, the  
3 values for instantaneous and equilibrium moduli measured from the MNC/NC-seeded  
4 constructs after 8 weeks of implantation were 8.4- and 17.4-fold lower, respectively,  
5 compared to human auricular cartilage (e.g.  $6.4 \pm 3.2$  MPa for  $E_{in}$  and  $3.3 \pm 1.3$  MPa for  $E_{eq}$   
6 [22]). Therefore, the engineered cartilage as such would not be suitable for immediate ear  
7 cartilage replacement; rather modifications in cell concentration and perhaps a longer  
8 implantation period needs to be considered.  
9

10 The present study has certain limitations. Firstly, cell density plays a critical role when  
11 engineering functional and stable cartilage. Others have demonstrated that cell densities  
12 greater than  $20 \times 10^6$  cells/ml are desirable, while low cell densities resulted in decreased  
13 cartilage formation [55]. During embryology of cartilage, densely packed and proliferative  
14 mesenchymal cells are responsible for depositing the vast amount of cartilage ECM. In  
15 cartilage TE, early phase of cartilage development needs to be simulated to generate  
16 functional and stable cartilage. Therefore, in order to enhance the outcome of tissue-  
17 engineered auricular cartilage, a higher cell density is needed to benefit from increased cell-  
18 cell contacts signaling chondrogenic ECM deposition and preventing the dedifferentiation  
19 process. Despite the limitations already stated, our findings support that bilayer BNC  
20 scaffolds in combination with alginate provide a suitable environment for MNCs and NCs to  
21 support the synthesis of neocartilage. Of equal importance, the use of freshly isolated human  
22 chondrocytes and mononuclear cells in the *in vivo* study gave us an indication of the potential  
23 of this strategy to advance the translation of cell-aided treatments to the clinic.  
24

25 Most auricular cartilage TE strategies have revolved around biodegradable scaffolds, where  
26 the hypothetical optimum has been the scaffold's degradation orchestrated by the neo-tissue  
27 formation. It would be ideal if the scaffold could be degraded by the time the neocartilage has  
28  
29  
30  
31  
32  
33  
34  
35  
36  
37  
38  
39  
40  
41  
42  
43  
44  
45  
46  
47  
48  
49  
50  
51  
52  
53  
54  
55  
56  
57  
58  
59  
60  
61  
62  
63  
64  
65

reached full mechanical strength. However, fine-tuning this intricate play has proven to be a challenge in TE. If the material degrades too rapidly, the neocartilage will collapse. Whereas if it degrades too late, it could induce a continuous inflammation that would affect the cartilage formation and when the material is finally degraded it would leave holes in the tissue, making it more prone to crack or collapse. Thus, we aim for a hybrid implant – BNC well integrated with the host and neo-tissue. The non-degradable BNC will provide long-term structural integrity after implantation, and has previously shown remarkable integration with the host tissue in different animal models [5, 6, 8, 56].

1  
2  
3  
4  
5  
6  
7  
8  
9  
10  
11  
12  
13  
14  
15  
16  
17  
18  
19  
20  
21  
22  
23  
24  
25  
26  
27  
28  
29  
30  
31  
32  
33  
34  
35  
36  
37  
38  
39  
40  
41  
42  
43  
44  
45  
46  
47  
48  
49  
50  
51  
52  
53  
54  
55  
56  
57  
58  
59  
60  
61  
62  
63  
64  
65

## Conclusions

1  
2 A novel BNC scaffold designed with a bilayer architecture that integrates mechanical  
3  
4 stability and high porosity was successfully fabricated and evaluated for auricular cartilage  
5  
6 TE, *in vitro* and *in vivo*. In conclusion, this study demonstrates that non-pyrogenic and non-  
7  
8 cytotoxic bilayer BNC scaffolds can be successfully produced. Furthermore, such scaffolds,  
9  
10 together with alginate, provide a suitable environment for culture-expanded human  
11  
12 nasoseptal chondrocytes and freshly isolated human nasoseptal chondrocytes combined with  
13  
14 freshly isolated human mononuclear cells to form cartilage *in vitro* and *in vivo*. Most studies  
15  
16 that have used biodegradable materials to engineer auricular cartilage have resulted in poor  
17  
18 structural integrity of the scaffold after implantation due to the short-lived chemical stability  
19  
20 of the scaffold material. This study found that bilayer BNC scaffolds offer a good mechanical  
21  
22 stability and maintain a structural integrity while providing a porous architecture that  
23  
24 supports cell ingrowth and neocartilage formation, as demonstrated by  
25  
26 immunohistochemistry, biochemical and biomechanical analyses. Ongoing work focuses on  
27  
28 developing bilayer BNC scaffolds in the shape of a human auricle, aiming to provide an  
29  
30 effective treatment to serious auricular defects.  
31  
32  
33  
34  
35  
36  
37  
38  
39  
40  
41  
42  
43  
44  
45  
46  
47  
48  
49  
50  
51  
52  
53  
54  
55  
56  
57  
58  
59  
60  
61  
62  
63  
64  
65



## Acknowledgements

1  
2 This study was performed within the framework of EuroNanoMed (EAREG-406340-  
3  
4 131009/1) and was supported by the Swedish Research Council (2009-7838), Federal  
5  
6 Ministry of Education and Research (13N11076), SenterNovem (ENM09001) and the Swiss  
7  
8 National Science Foundation (NRP63). The authors acknowledge Dr. Annette Jork and  
9  
10 CellMed AG (Alzenau, Germany) for providing medical grade alginate; Athanasios Mantas  
11  
12 and Anders Mårtensson at Chalmers University of Technology (Gothenburg, Sweden) for  
13  
14 assistance with scaffold production and FTIR analysis, respectively; and Priscila Martínez  
15  
16  
17  
18  
19  
20  
21  
22  
23  
24  
25  
26  
27  
28  
29  
30  
31  
32  
33  
34  
35  
36  
37  
38  
39  
40  
41  
42  
43  
44  
45  
46  
47  
48  
49  
50  
51  
52  
53  
54  
55  
56  
57  
58  
59  
60  
61  
62  
63  
64  
65

Ávila at The University of Texas at Arlington for helping with statistical analysis. The antibody used for immunohistochemical type II collagen detection (II-II6B3) was obtained from the Developmental Studies Hybridoma Bank, created by the NICHD of the NIH and maintained at the University of Iowa, Department of Biology, Iowa City, IA 52242, USA.

## References

- [1] Bichara DA, O'Sullivan NA, Pomerantseva I, Zhao X, Sundback CA, Vacanti JP, et al. The tissue-engineered auricle: past, present, and future. *Tissue Eng Part B Rev.* 2012;18:51-61.
- [2] Tanzer RC. Total reconstruction of the auricle. The evolution of a plan of treatment. *Plast Reconstr Surg.* 1971;47:523-33.
- [3] Persichetti P, Piombino L, Toto V, Segreto F, Marangi GF. Septal cartilage graft for posttraumatic ear reconstruction. *Plast Reconstr Surg.* 2011;128:773e-5e.
- [4] Mello LR, Feltrin LT, Neto PTF, Ferraz FAP. Duraplasty with biosynthetic cellulose: An experimental study. *J Neurosurg.* 1997;86:143-50.
- [5] Helenius G, Bäckdahl H, Bodin A, Nannmark U, Gatenholm P, Risberg B. In vivo biocompatibility of bacterial cellulose. *J Biomed Mater Res A.* 2006;76:431-8.
- [6] Andrade FK, Alexandre N, Amorim I, Gartner F, Mauricio AC, Luis AL, et al. Studies on the biocompatibility of bacterial cellulose. *J Bioact Compat Pol.* 2013;28:97-112.
- [7] Pertile RA, Moreira S, Costa RM, Correia A, Guardao L, Gartner F, et al. Bacterial Cellulose: Long-Term Biocompatibility Studies. *J Biomater Sci Polym Ed.* 2011.
- [8] Martínez Ávila H, Schwarz S, Feldmann E-M, Mantas A, von Bomhard A, Gatenholm P, et al. Biocompatibility evaluation of densified bacterial nanocellulose hydrogel as an implant material for auricular cartilage regeneration. *Appl Microbiol Biotechnol.* 2014;98:7423-35.
- [9] Svensson A, Nicklasson E, Harrah T, Panilaitis B, Kaplan DL, Brittberg M, et al. Bacterial cellulose as a potential scaffold for tissue engineering of cartilage. *Biomaterials.* 2005;26:419-31.
- [10] Ahrem H, Pretzel D, Endres M, Conrad D, Courseau J, Muller H, et al. Laser-structured bacterial nanocellulose hydrogels support ingrowth and differentiation of chondrocytes and show potential as cartilage implants. *Acta Biomater.* 2014;10:1341-53.
- [11] Bäckdahl H, Helenius G, Bodin A, Nannmark U, Johansson BR, Risberg B, et al. Mechanical properties of bacterial cellulose and interactions with smooth muscle cells. *Biomaterials.* 2006;27:2141-9.
- [12] Zaborowska M, Bodin A, Bäckdahl H, Popp J, Goldstein A, Gatenholm P. Microporous bacterial cellulose as a potential scaffold for bone regeneration. *Acta Biomaterialia.* 2010;6:2540-7.
- [13] Martínez Ávila H, Brackmann C, Enejder A, Gatenholm P. Mechanical stimulation of fibroblasts in micro-channeled bacterial cellulose scaffolds enhances production of oriented collagen fibers. *J Biomed Mater Res A.* 2012;100:948-57.
- [14] Feldmann EM, Sundberg J, Bobbili B, Schwarz S, Gatenholm P, Rotter N. Description of a novel approach to engineer cartilage with porous bacterial nanocellulose for reconstruction of a human auricle. *J Biomater Appl.* 2013.
- [15] Bodin A, Bharadwaj S, Wu SF, Gatenholm P, Atala A, Zhang YY. Tissue-engineered conduit using urine-derived stem cells seeded bacterial cellulose polymer in urinary reconstruction and diversion. *Biomaterials.* 2010;31:8889-901.
- [16] Deinema M, Zevenhuizen LPTM. Formation of cellulose fibrils by gram-negative bacteria and their role in bacterial flocculation. *Arch Mikrobiol.* 1971;78:42-57.
- [17] Brown RM, Jr., Willison JH, Richardson CL. Cellulose biosynthesis in *Acetobacter xylinum*: visualization of the site of synthesis and direct measurement of the in vivo process. *Proc Natl Acad Sci U S A.* 1976;73:4565-9.
- [18] Fink HP, Purz HJ, Bohn A, Kunze J. Investigation of the supramolecular structure of never dried bacterial cellulose. *Macromol Symp.* 1997;120:207-17.

- 1 [19] Czaja WK, Young DJ, Kawecki M, Brown RM. The future prospects of microbial  
2 cellulose in biomedical applications. *Biomacromolecules*. 2007;8:1-12.
- 3 [20] Gatenholm P, Klemm D. Bacterial Nanocellulose as a Renewable Material for  
4 Biomedical Applications. *MRS Bulletin*. 2010;35:208-13.
- 5 [21] Petersen N, Gatenholm P. Bacterial cellulose-based materials and medical devices:  
6 current state and perspectives. *Appl Microbiol Biot*. 2011;91:1277-86.
- 7 [22] Nimeskern L, Martínez Ávila H, Sundberg J, Gatenholm P, Müller R, Stok KS.  
8 Mechanical evaluation of bacterial nanocellulose as an implant material for ear cartilage  
9 replacement. *J Mech Behav Biomed*. 2013;22:12-21.
- 10 [23] Lee SJ, Broda C, Atala A, Yoo JJ. Engineered cartilage covered ear implants for  
11 auricular cartilage reconstruction. *Biomacromolecules*. 2011;12:306-13.
- 12 [24] Yanaga H, Imai K, Fujimoto T, Yanaga K. Generating Ears from Cultured Autologous  
13 Auricular Chondrocytes by Using Two-Stage Implantation in Treatment of Microtia. *Plast*  
14 *Reconstr Surg*. 2009;124:817-25 10.1097/PRS.0b013e3181b17c0e.
- 15 [25] Zhou L, Pomerantseva I, Bassett EK, Bowley CM, Zhao X, Bichara DA, et al.  
16 Engineering ear constructs with a composite scaffold to maintain dimensions. *Tissue Eng*  
17 *Part A*. 2011;17:1573-81.
- 18 [26] Nimeskern L, van Osch GJ, Muller R, Stok KS. Quantitative evaluation of mechanical  
19 properties in tissue-engineered auricular cartilage. *Tissue Eng Part B Rev*. 2014;20:17-27.
- 20 [27] Cao Y, Vacanti JP, Paige KT, Upton J, Vacanti CA. Transplantation of chondrocytes  
21 utilizing a polymer-cell construct to produce tissue-engineered cartilage in the shape of a  
22 human ear. *Plast Reconstr Surg*. 1997;100:297-302; discussion 3-4.
- 23 [28] Haisch A, Klaring S, Groger A, Gebert C, Sittinger M. A tissue-engineering model for  
24 the manufacture of auricular-shaped cartilage implants. *Eur Arch Otorhinolaryngol*.  
25 2002;259:316-21.
- 26 [29] Isogai N, Asamura S, Higashi T, Ikada Y, Morita S, Hillyer J, et al. Tissue engineering  
27 of an auricular cartilage model utilizing cultured chondrocyte-poly(L-lactide-epsilon-  
28 caprolactone) scaffolds. *Tissue Eng*. 2004;10:673-87.
- 29 [30] Kusuhara H, Isogai N, Enjo M, Otani H, Ikada Y, Jacquet R, et al. Tissue engineering a  
30 model for the human ear: assessment of size, shape, morphology, and gene expression  
31 following seeding of different chondrocytes. *Wound Repair Regen*. 2009;17:136-46.
- 32 [31] Shieh SJ, Terada S, Vacanti JP. Tissue engineering auricular reconstruction: in vitro and  
33 in vivo studies. *Biomaterials*. 2004;25:1545-57.
- 34 [32] Ruzsyzmah BHI, Chua KH, Mazlyzam AL, Aminuddin BS. Formation of tissue  
35 engineered composite construct of cartilage and skin using high density polyethylene as inner  
36 scaffold in the shape of human helix. *International journal of pediatric otorhinolaryngology*.  
37 2011;75:805-10.
- 38 [33] Béguin P, Aubert J-P. The biological degradation of cellulose. *FEMS Microbiology*  
39 *Reviews*. 1994;13:25-58.
- 40 [34] Martínez Ávila H, Sundberg J, Prakash S, Seniger M, Gatenholm P. Bioprinting of 3D  
41 patient-specific auricular scaffolds. *J Tissue Eng Regen Med*. 2012;6:153.
- 42 [35] Bäckdahl H, Esguerra M, Delbro D, Risberg B, Gatenholm P. Engineering  
43 microporosity in bacterial cellulose scaffolds. *J Tissue Eng Regen Med*. 2008;2:320-30.
- 44 [36] Chiaoprakobkij N, Sanchavanakit N, Subbalekha K, Pavasant P, Phisalaphong M.  
45 Characterization and biocompatibility of bacterial cellulose/alginate composite sponges with  
46 human keratinocytes and gingival fibroblasts. *Carbohydrate Polymers*. 2011;85:548-53.
- 47 [37] Sundberg J, Feldmann E, Martinez H, Schwarz S, Rotter N, Gatenholm P. Evaluation of  
48 macroporous bacterial nanocellulose scaffolds for ear cartilage tissue engineering. In: *Tissue*  
49 *Engineering and Regenerative Medicine International Society World Congress, Vienna,*  
50 *Austria, September 5-8, 2012. J Tissue Eng Regen Med*. 2012;6 (Suppl. 1):1-429.
- 51  
52  
53  
54  
55  
56  
57  
58  
59  
60  
61  
62  
63  
64  
65

- 1 [38] Andersson J, Stenhamre H, Bäckdahl H, Gatenholm P. Behavior of human chondrocytes  
2 in engineered porous bacterial cellulose scaffolds. *J Biomed Mater Res A*. 2010;94:1124-32.
- 3 [39] Pleumeekers MM, Nimeskern L, Koevoet WL, Kops N, Poublon RM, Stok KS, et al.  
4 The in vitro and in vivo capacity of culture-expanded human cells from several sources  
5 encapsulated in alginate to form cartilage. *Eur Cell Mater*. 2014;27:264-80; discussion 78-80.
- 6 [40] de Windt TS, Hendriks JA, Zhao X, Vonk LA, Creemers LB, Dhert WJ, et al. Concise  
7 review: unraveling stem cell cocultures in regenerative medicine: which cell interactions steer  
8 cartilage regeneration and how? *Stem Cells Transl Med*. 2014;3:723-33.
- 9 [41] Hendriks JAA, Riesle JU, Wilson CE, Van Den Doel MA. Cartilage cell processing  
10 system. In: Office USPaT, editor. USPTOgov. US: Cellcotec B.V.; 2014.
- 11 [42] Häuselmann HJ, Fernandes RJ, Mok SS, Schmid TM, Block JA, Aydelotte MB, et al.  
12 Phenotypic stability of bovine articular chondrocytes after long-term culture in alginate  
13 beads. *J Cell Sci*. 1994;107 ( Pt 1):17-27.
- 14 [43] Matsuoka M TT, Matsushita K, Adachi O, Yoshinaga F. A synthetic medium for  
15 bacterial cellulose production by *Acetobacter xylinum* subsp. sucrofermentation. *Biosci*  
16 *Biotechnol Biochem*. 1996;60:575-9.
- 17 [44] Nimeskern L, Feldmann E-M, Kuo W, Schwarz S, Goldberg-Bockhorn E, Dürr S, et al.  
18 Magnetic Resonance Imaging of the Ear for Patient-Specific Reconstructive Surgery. *PLoS*  
19 *One*. 2014;9:e104975.
- 20 [45] Bouxsein ML, Boyd SK, Christiansen BA, Guldborg RE, Jepsen KJ, Muller R.  
21 Guidelines for assessment of bone microstructure in rodents using micro-computed  
22 tomography. *J Bone Miner Res*. 2010;25:1468-86.
- 23 [46] FDA US. Guidance for Industry - Pyrogen and Endotoxins Testing: Questions and  
24 Answers. In: Services USDoHH, editor. Silver Spring: U.S. Food and Drug Administration;  
25 June 2012. p. 8.
- 26 [47] Hierck BP, Iperen LV, Gittenberger-De Groot AC, Poelmann RE. Modified indirect  
27 immunodetection allows study of murine tissue with mouse monoclonal antibodies. *J*  
28 *Histochem Cytochem*. 1994;42:1499-502.
- 29 [48] Enobakhare BO, Bader DL, Lee DA. Quantification of sulfated glycosaminoglycans in  
30 chondrocyte/alginate cultures, by use of 1,9-dimethylmethylene blue. *Anal Biochem*.  
31 1996;243:189-91.
- 32 [49] Stok KS, Lisignoli G, Cristino S, Facchini A, Muller R. Mechano-functional assessment  
33 of human mesenchymal stem cells grown in three-dimensional hyaluronan-based scaffolds  
34 for cartilage tissue engineering. *J Biomed Mater Res A*. 2010;93:37-45.
- 35 [50] Dhumal NR, Kim HJ, Kiefer J. Molecular interactions in 1-ethyl-3-methylimidazolium  
36 acetate ion pair: a density functional study. *J Phys Chem A*. 2009;113:10397-404.
- 37 [51] Viell J, Marquardt W. Concentration measurements in ionic liquid-water mixtures by  
38 mid-infrared spectroscopy and indirect hard modeling. *Applied Spectroscopy*. 2012;66:208-  
39 17.
- 40 [52] Chen H-L, Kao H-F, Wang J-Y, Wei G-T. Cytotoxicity of Imidazole Ionic Liquids in  
41 Human Lung Carcinoma A549 Cell Line. *J Chin Chem Soc-Taip*. 2014;61:763-9.
- 42 [53] Marijnissen WJ, van Osch GJ, Aigner J, van der Veen SW, Hollander AP, Verwoerd-  
43 Verhoef HL, et al. Alginate as a chondrocyte-delivery substance in combination with a non-  
44 woven scaffold for cartilage tissue engineering. *Biomaterials*. 2002;23:1511-7.
- 45 [54] Marijnissen WJ, van Osch GJ, Aigner J, Verwoerd-Verhoef HL, Verhaar JA. Tissue-  
46 engineered cartilage using serially passaged articular chondrocytes. Chondrocytes in alginate,  
47 combined in vivo with a synthetic (E210) or biologic biodegradable carrier (DBM).  
48 *Biomaterials*. 2000;21:571-80.
- 49  
50  
51  
52  
53  
54  
55  
56  
57  
58  
59  
60  
61  
62  
63  
64  
65

1 [55] Puelacher WC, Kim SW, Vacanti JP, Schloo B, Mooney D, Vacanti CA. Tissue-  
2 engineered growth of cartilage: the effect of varying the concentration of chondrocytes  
3 seeded onto synthetic polymer matrices. *Int J Oral Maxillofac Surg.* 1994;23:49-53.

4 [56] Malm CJ, Risberg B, Bodin A, Bäckdahl H, Johansson BR, Gatenholm P, et al. Small  
5 calibre biosynthetic bacterial cellulose blood vessels: 13-months patency in a sheep model.  
6 *Scandinavian Cardiovascular Journal.* 2012;46:57-62.  
7  
8  
9  
10  
11  
12  
13  
14  
15  
16  
17  
18  
19  
20  
21  
22  
23  
24  
25  
26  
27  
28  
29  
30  
31  
32  
33  
34  
35  
36  
37  
38  
39  
40  
41  
42  
43  
44  
45  
46  
47  
48  
49  
50  
51  
52  
53  
54  
55  
56  
57  
58  
59  
60  
61  
62  
63  
64  
65

## Figure captions

**Figure 1:** Fabrication and purification process of bilayer BNC scaffolds composed of a dense nanocellulose layer joined with a macroporous composite layer. BNC hydrogel disks with cellulose content of 17% (i.e. dense layer) were produced by compression, whereas BNC/alginate composite scaffolds (i.e. porous layer) were fabricated by a freeze-drying process. A novel cellulose solvent system (i.e. ionic liquid EMIMAc) was used to achieve a strong interfacial molecular bonding between the dense and porous layers. The bilayer BNC scaffolds were then washed with endotoxin-free water for 14 days to yield non-pyrogenic and non-cytotoxic scaffolds.

**Figure 2:** (a) Photograph of bilayer BNC scaffold (side view). Comparison between (b, c) scanning electron microscopy images of bilayer BNC scaffolds and (d) 3D reconstructed model of the porous layer using microtomography. Similar honeycomb arrangement of sheet-like structures is visible in both images. (e) Higher magnification of the area marked red in (d). Morphometric analysis of segmented porous layer: (f) Morphometric parameters (Sc.Po: scaffold porosity, Pore.Th: volume-weighted mean pore size, Wall.Th: scaffold wall thickness, and Wall.N: scaffold wall number) and (g) Histogram of pore size distribution.

**Figure 3:** (a) ATR spectra of (1) 1-Ethyl-3-methylimidazolium acetate (EMIMAc); bilayer BNC scaffolds after (2) 1 day, (3) 7 days and (4) 14 days of purification in endotoxin-free water; and (5) pure bacterial nanocellulose (BNC). (b) *In vitro* cytotoxicity testing of bilayer BNC scaffolds after 7 and 14 days of purification in endotoxin-free water ( $n=4$  per time point). Post hoc comparisons using the Tukey HSD test indicated that the mean cell viability for the 14-day condition ( $97.8 \pm 4.7\%$ ) was significantly higher than the 7-day ( $18.4 \pm 3.6\%$ ) and positive control conditions ( $25.6 \pm 5.5\%$ ) at the  $*p<0.05$  level. Furthermore, there was no significant difference between the negative control and 14-day conditions. Thus, the cytotoxic potential of bilayer BNC scaffolds after 14 days of purification was classified as non-cytotoxic (cell viability  $> 71\%$ ). Error bars represent the standard deviation of the mean.

**Figure 4:** Histological and immunohistochemical analysis of human nasoseptal chondrocytes after 2, 4 and 6 weeks of culture *in vitro* in chondrogenic medium. Representative images of ECM produced in bilayer bacterial nanocellulose (BNC) scaffolds. Samples were stained with (a) Alcian blue to detect deposition of sulfated glycosaminoglycans (*PL = porous layer*). Immunohistochemical staining was used to detect cartilage specific proteins such as (b) aggrecan, (c) type II collagen and (d) the dedifferentiation marker type I collagen. (e and f) Gene expression analysis of human nasoseptal chondrocytes seeded in bilayer BNC scaffolds and cultured *in vitro* for 2, 4 and 6 weeks ( $n=4$  per time point). Gene expression levels of *ACAN*, *COL2A1*, *COL1A1* and *VCAN* relative to the housekeeping gene Glyceraldehyde 3-phosphate dehydrogenase (*GAPDH*). Error bars represent the standard deviation of the mean. The scale bar indicates 1 mm (a-d).

**Figure 5:** (a) Photographs of cell-free and MNC/NC-seeded bilayer BNC scaffolds after 8 weeks of subcutaneous implantation in nude mice. Histological evaluation of ECM in bilayer bacterial nanocellulose (BNC) scaffolds seeded with a combination of freshly isolated nasoseptal chondrocytes (NC) and bone marrow mononuclear cells (MNC) in alginate after 8 weeks of subcutaneous implantation. (b) Safranin O stain was used to examine proteoglycans present in the newly synthesized ECM, (c) whereas immunohistochemical analysis was used to detect type II collagen. (d) Cell-free and MNC/NC-seeded bilayer BNC scaffolds were also analyzed for glycosaminoglycan (GAG) content after 8 weeks of subcutaneous implantation ( $n=4$  per group). A two-sample Kolmogorov-Smirnov test indicated a significant difference between mean GAG content for MNC/NC-seeded ( $0.87 \pm 0.65 \mu\text{g GAG/mg wet weight}$ ) and cell-free bilayer BNC scaffolds ( $0.07 \pm 0.11 \mu\text{g GAG/mg wet weight}$ ). (e) Biomechanical evaluation of cell-free and MNC/NC-seeded constructs after 8 weeks of subcutaneous implantation ( $n=4$  per group), and non-implanted bilayer BNC scaffolds with cell-free alginate solution ( $n=5$ ). Post hoc comparisons using the Tukey HSD test indicated that the mean  $E_{in}$  for the MNC/NC condition ( $0.76 \pm 0.19$  MPa) was significantly higher than the non-implanted ( $0.42 \pm 0.15$  MPa) and cell-free conditions ( $0.32 \pm 0.10$  MPa). Moreover, post hoc comparisons using the Mann-Whitney tests indicated that the median  $t_{1/2}$  for the MNC/NC condition was significantly higher than the non-implanted ( $U = 3$ ,  $p<0.001$ ,  $r = -0.74$ ) and cell-free conditions ( $U = 48$ ,  $p<0.01$ ,  $r = -0.66$ ). Error bars represent the standard deviation of the mean. \*, \*\* or \*\*\* indicates  $p$ -values less than 0.05, 0.01 or 0.001, respectively. The scale bars indicate 4 mm (a) and 1 mm (b, c).

## Tables

**Table 1: Sequences of target genes and reference gene for real-time two-step RT-PCR.**

	UPL probe #	Sense primer	Antisense primer	Amplicon (nt)
<b>Target genes</b>				
<i>ACAN</i>	79	5'-tgcagctgtcactgtagaaactt-3'	5'-atagcaggggatggtgagg-3'	112
<i>COL1A1</i>	15	5'-atgttcagcttggacctc-3'	5'-ctgtacgcaggtgattggtg-3'	126
<i>COL2A1</i>	19	5'-ccctggctctggtggaac-3'	5'-tcctgcattactccaactg-3'	88
<i>VCAN</i>	54	5'-gcacctgtgtgccaggata-3'	5'-cagggattagagtgcattcatca-3'	70
<b>Housekeeping gene</b>				
<i>GAPDH</i>	60	5'-gctctctgctcctcctgttc-3'	5'-acgaccaaatccgttgactc-3'	115

**Table 2: Results from bacterial endotoxin testing. Assay sensitivity 0.005 Endotoxin Units per ml (EU/ml). Valid test parameter: each sample is tested with a positive product control (PPC) of 0.1 EU/ml. If the spike recovery is between 50-200 % of the PPC, the result is valid.**

Sample #	Dilution	Results (EU/ml)	Spike recovery (%)	Status	Mean ± SD (EU/ml)
1	1/10	0.26	59	Valid	0.15 ± 0.09
2	1/10	0.10	90	Valid	
3	1/10	0.10	55	Valid	

Figure1

[Click here to download high resolution image](#)

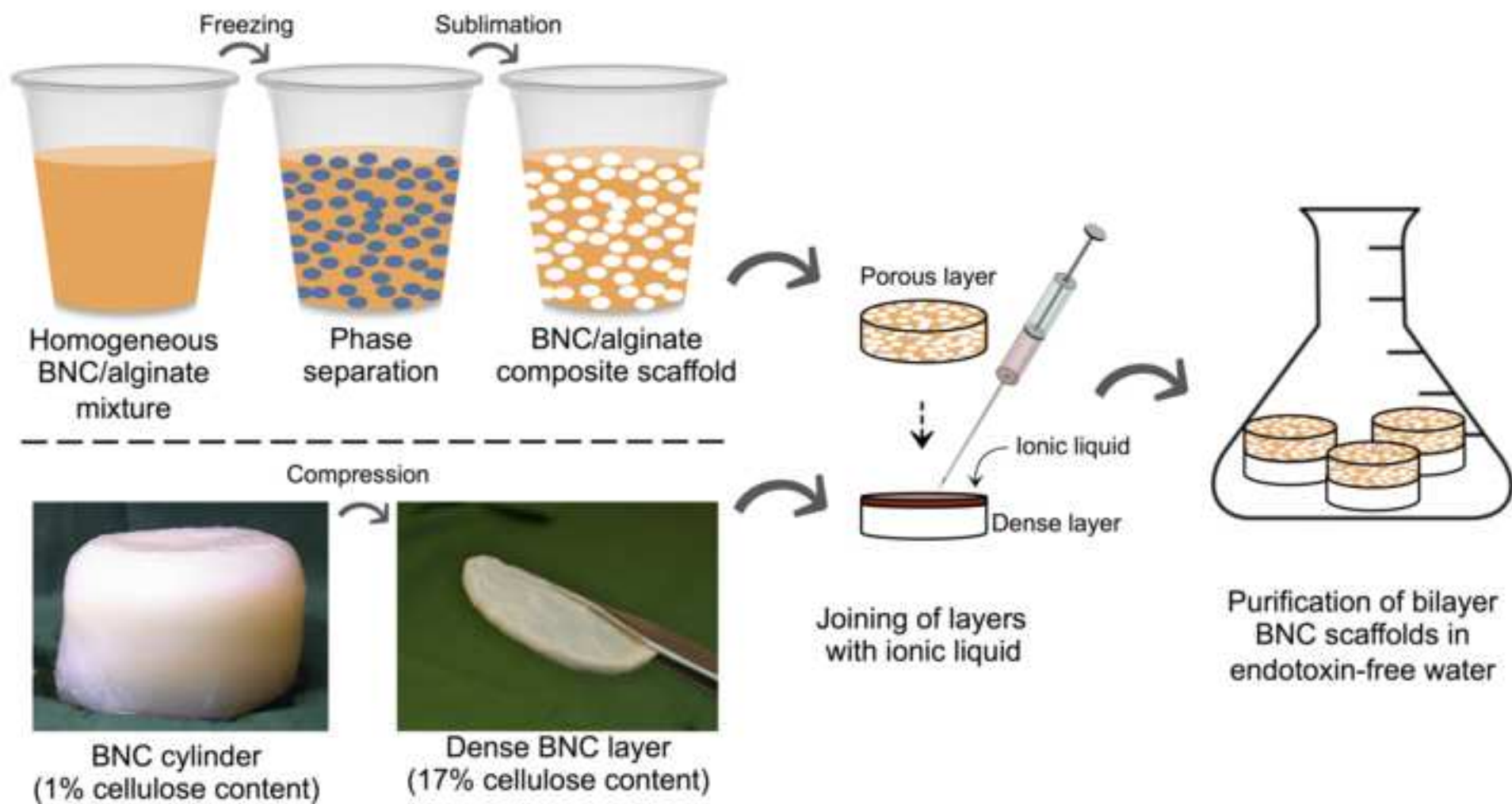




Figure2  
[Click here to download high resolution image](#)

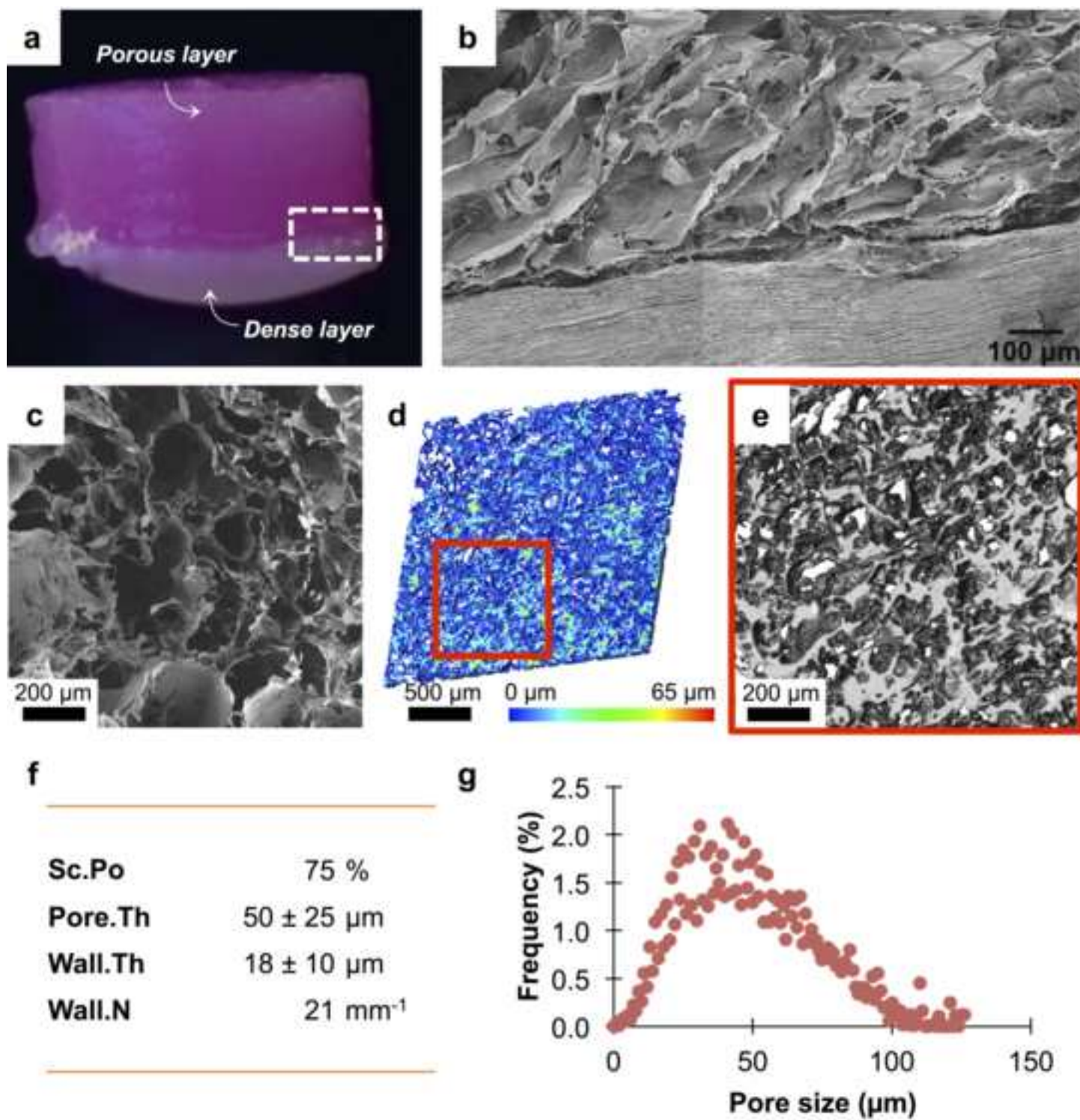


Figure3  
[Click here to download high resolution image](#)

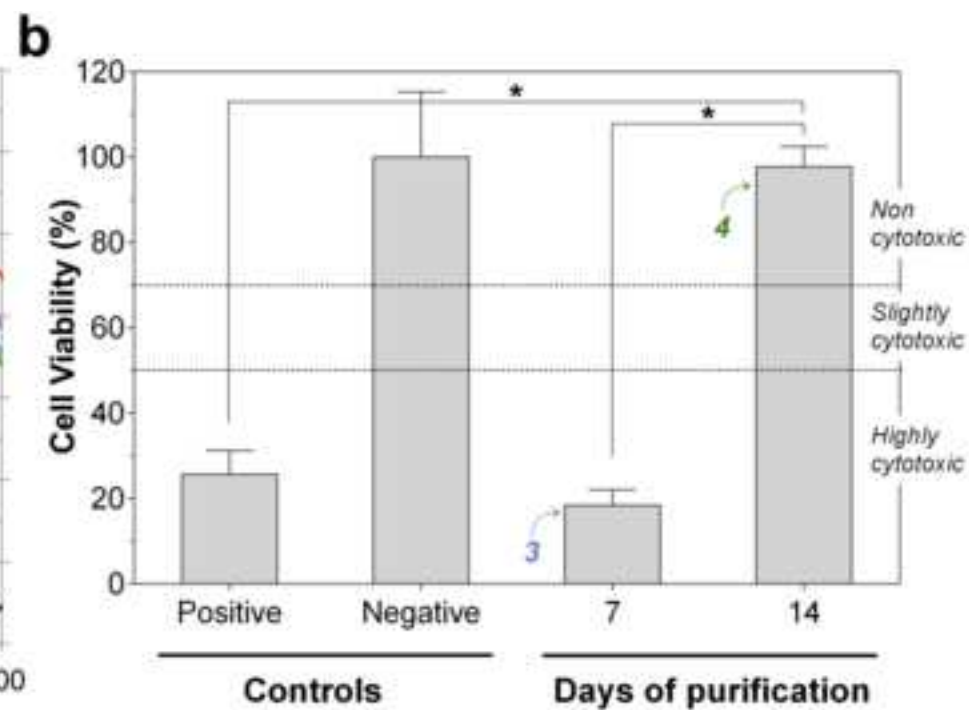
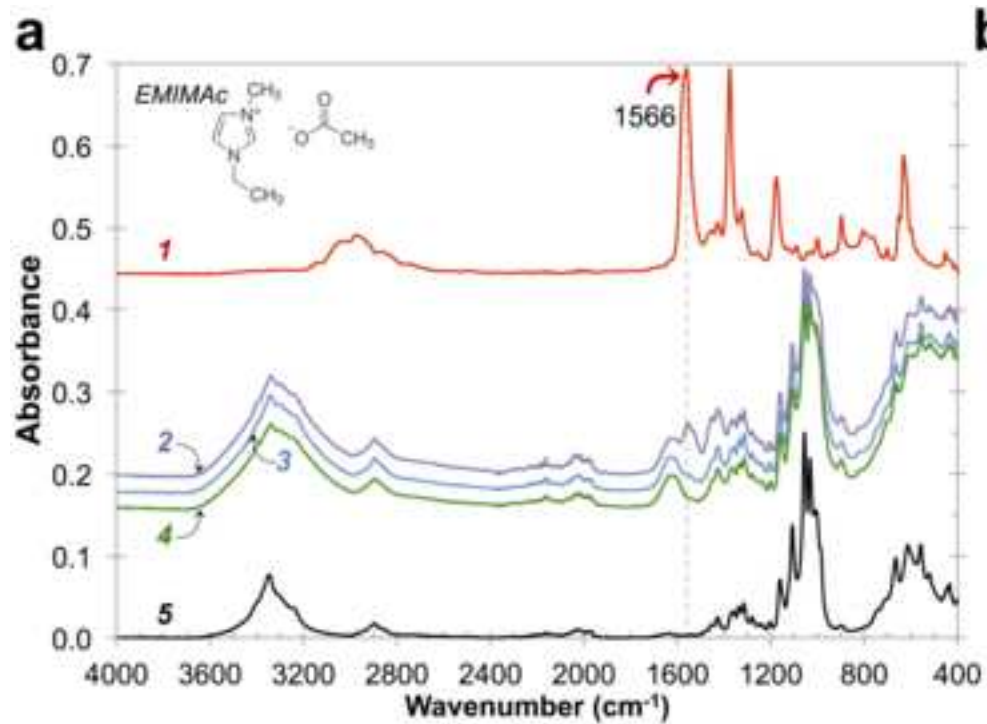


Figure4

[Click here to download high resolution image](#)

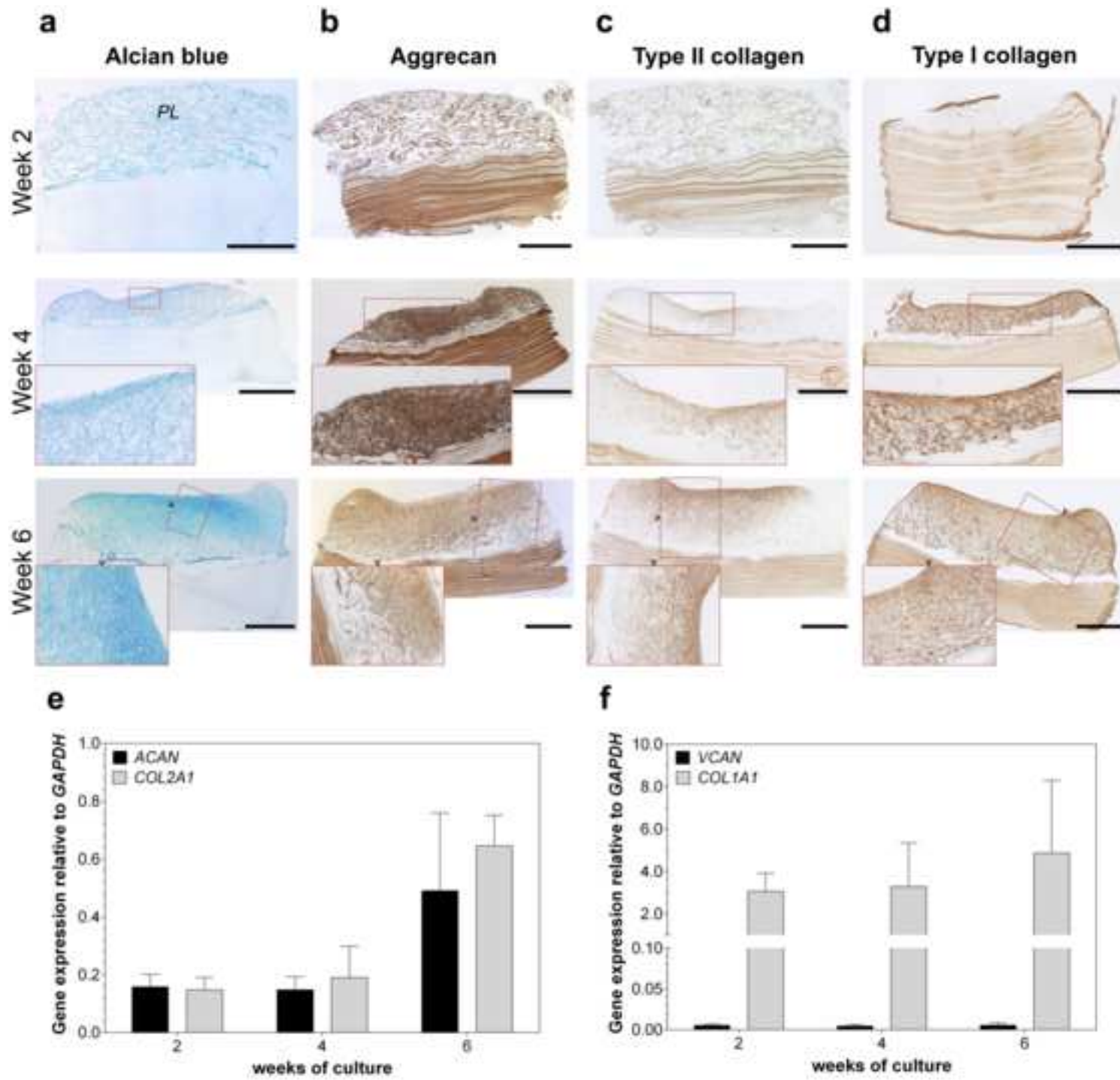


Figure5  
[Click here to download high resolution image](#)

